Environ Monit Assess (2023) 195:1053
https://doi.org/10.1007/s10661-023-11630-x

RESEARCH

Assessing the status and spatial-temporal dynamics of the Bamenda Mountains (BM), North West region of Cameroon

Virgiline Kongni Fopa · **Nihal Bayir** ·
Devrim ÖZDAL

Received: 3 December 2022 / Accepted: 22 July 2023 / Published online: 17 August 2023
© The Author(s), under exclusive licence to Springer Nature Switzerland AG 2023

Abstract Change in land use and land cover (LULC) contributes in worsening ecological issues. Studying the trends of change in land use is highly significant to deal with global climate change and sustainable development. The aim of this paper is to evaluate the spatial-temporal dynamics of LULC of the Bamenda Mountains (BM) in the North West region of Cameroon, over a period of 34 years (1988–2022) and predict 34 years (2022–2056) future land use scenario of this site using time series satellite imagery (MSS, TM, ETM+, and OLI-TIRS) and ancillary data and to comprehend the driving forces of land use/land cover change (LULCC). The trends of LULCC were quantified; LULC maps were derived by classifying time series satellite images. Six LULC categories were identified during the study period (1988–2022). The research revealed a significant LULCC of the BM which can be justified by increase in the human population observed in the study area and the desire to extend agricultural lands to sustain the growing population. Overall, cultivated area 5684 ha (10.47%), 10680 ha (19.57 %), and 15163 ha (27.78%) and built-up area 449 ha (0.83%), 996 ha (1.83%), and 3242 ha (5.94%) for the study years 1988, 2003, and 2022, respectively, were all on the increase throughout the study period at the expense of other land cover types. The predicted figures of 2056 showed a continuous reduction of montane forest and savanna: 2401.92 ha (4.40%) and 25,862.67 ha (47.39%), respectively. Bare area is expected to drop in 2056 (2905.92 ha (5.32%)). The above decrease, when compared to 2022 figures, represents a loss of 3.97%, 4.53%, and 0.57%, respectively. The losses observed are gained by built-up and cultivated land (5.72% and 3.39%, respectively), covering surfaces areas of 6364.89 ha (11.66%) and 17,008.56 ha (31.17%), respectively. The above findings suggest that population growth is likely the major menace to the natural environment. It is thus safe to say that substantial LULCC was observed throughout the study period and will undoubtedly continue if nothing is done. This necessitates urgent measures such as reforestation and afforestation, encouraging off-farm activities and even improving technologies to combat the rate of forest degradation of the BM. Additionally, rebuilding trust between the French and English Cameroons through dialogue is premodial, to end the

V. K. Fopa (✉)
Department of Environmental Sciences, Institute of Graduate Studies and Research, European University of Lefke, Northern Cyprus TR-10, 99010 Mersin, Turkey
e-mail: fopavirgiline@gmail.com

N. Bayir
Chemical Engineering Program, Middle East Technical University, Northern Cyprus Campus, 10, 99738 Mersin, Turkey
e-mail: bayir@metu.edu.tr

D. ÖZDAL
Department of Environmental Sciences, Faculty of Engineering, European University of Lefke, Northern Cyprus TR-10, 99010 Mersin, Turkey
e-mail: devrimozdal@eul.edu.tr

curent conflictual civil war and lessen the landscape configuration in Bamenda.

Keywords LULC change · Change prediction · GIS · Remote sensing · Mount Bamenda(BM)

Introduction

Land use and land cover change (LULCC) has been an alarming situation in both developed and less developed countries of the world, due to their repercussions on sustainable development and far reaching effects on other segments of the economy. For the past years, land resource has always been closely associated with economic, social, and other anthropogenic activities (Alemayehu et al., 2019). The patterns of land use and land cover (LULC) of a place is thus the result of the socio-economic, natural factors, and their spatiotemporal utilization by humans. LULC dynamics are extended and accelerated with the main driving force being population growth. These landscape alterations play a significant role in natural resource deterioration and have repercussions on man (Leh et al., 2013; Alemayehu et al., 2019; Chen et al., 2022).

The world population is growing at a speedy rate, and recent forecasts suggest that the planet may contain 9.8 billion people by 2050 or 11. 2 billion people by 2100 (DESA, 2017). This implies that urban growth will have broad effects on environmental, social, and economic services that mankind heavily relies on (Mattsson et al., 2022). Continuous encroachment on the land use and land cover has an important impact on ecosystems with a great influence on the diversity of the biotic and abiotic components of the ecosystem as well as the ability of the landscapes and humans to cope with climatic, socioeconomic, and political disturbances. It is therefore necessary to be knowledgeable about these superficial processes to forecast future scenarios to ensure sustainable development (Kibreab, 1996; Ahlcrona, 1989; Olagunju, 2008).

LULCC can affect the energy balance, soil fertility, and the biogeochemical cycles. A constant watch and prediction of the changes are therefore necessary to ensure the environment is managed sustainably (Lupo et al., 2001; Kindu et al., 2013). Population pressure and other significant drivers such as government policies and poverty have accelerated the LULC dynamics of tropical mountains and have paved a way to tropical ecosystems losses (Kidane et al., 2012; Said et al., 2021). This goes against the 2030 Agenda, where the UN (United Nations) established its Sustainable Development Goal 15 aimed to "Protect, restore and promote sustainable use of terrestrial ecosystems, sustainably manage forests, combat desertification, and halt and reverse land degradation and halt biodiversity loss." Sustainable Mountain Development is also a major object of interest of Chapter 13 of Agenda 21, which stipulates that mountains are great sources of water, energy, biodiversity, agricultural products, and minerals (Maghah et al., 2021; Sachs et al., 2022; Jan et al., 2023).

Mountain ecosystems are rapidly degraded although they are sources of many water bodies, energy, biodiversity hotspots, and food reservoirs for humankind (FAO, 2017). These unique milieus sustain the population around and even beyond the mountains by regulating the quality and quantity of water originating therein. Mountain ecosystems are global assets but constantly threatened by anthropogenic activities and to an extent by natural disturbances (Gratzer & Keeton, 2017; Maghah et al., 2021).

The Bamenda Mountains (BM) in the North West region of Cameroon is a unique ecosystem and home to diverse flora and fauna of promising potentials. Animal rearing and agriculture are the principal activities influencing the livelihood and the economic well-being of the local population of the Mezam division in the North West region of Cameroon (Awazi, 2022). Mountainous forests being vulnerable are constantly degraded due to pressure from anthropogenic activities and natural disturbances. Forest degradation is generally a gradual process within the forest that adversely alters its characteristics, which affects the forest quality, there by compromising its ability to generate goods and services for mankind and the ecosystem. Forest lands can be altered both directly through overexploitation, overgrazing, and crude agricultural systems and indirectly through climate variability, epidemic, and landslide (Simula, 2009).

Few studies have analyzed land use/land cover change and their drivers (meanly anthropogenic activities) in Cameroon and in the north west region (Mofor et al., 2022; Maghah et al., 2021; Ntangti et al., 2019; Asaha et al., 2016; Ewane, 2021;

Asong et al., 2019; Temgoua et al., 2018). Meanwhile, a study by Forboseh et al. (2003) monitored bird species at Kilum Ijim Mountain Forest reserve to uncover the status of the forest and the individual species, thus considering suites of bird species as indicators of vegetation changes. However, no studies considered analyzing both the driving forces of LULCC and forecasting the future land use scenario of the Bamenda Mountains. The conversion of the initial land cover (vegetation) of the Bamenda Mountains to other land cover types notably built-up and agricultural land is mainly to sustain the growing population.

This study utilized remote sensing and GIS technology, based on time series satellite images to analyze the LULCC of the Bamenda Mountains and change prediction of this site using Markov chain model. This was initiated to inform policymakers and ensure the sustainable management of this site. The Markov chain model (MCM) for time series analysis and prediction used in this study is a stochastic model, modeling temporal or sequential data. This model predicts the future state of a system basing on the immediately preceding state and has been extensively used to model areas of land use changes at great spatial scales (Huang et al., 2008; Tadese et al., 2021).

Remote sensing is a competitive and cost-effective technology used to map out and obtain information from large portions of the earth. GIS and the remote sensing technology are efficient in mapping and analyzing land use changes and the mineral resources distribution, (Ahlcrona, 1989; Tematio, 2016) using multi-spectral scanner (MSS), thematic mapper (TM), and enhanced thematic mapper (ETM) data from Landsat satellite images. This technology has been used in many studies to identify features of land use and land cover changes and detect soil degradation activities (Mainguet, 2012; Leumbe et al., 2012). Quality image resolution makes it possible to monitor, analyze, and interpret land use changes for different periods of time to know the trends, the reasons, and the manner in which the changes occur (Rindfuss et al., 2004; Shiferaw & Singh, 2011).

As a prelude to the Bamenda Mountains forest resource conservation, vis-à-vis its indiscriminate exploitation, it is worth taking actions for the sustainable management of this site for the next generations to enjoy similar good and services offered.

The aim of this paper is to evaluate the spatial and temporal dynamics of LULC of the Bamenda Mountains (BM) in the North West region of Cameroon, over a period of 34 years (1988–2022) and predict 34 years (2022–2056) future land use scenario of this site using time series satellite imagery (TM, ETM+, and OLI-TIRS) and ancillary data and to understand the driving forces of the LULCC. The present research paper provides the entire Mezam division (North West region of Cameroon) and policymakers with the present and the future views of the Bamenda Mountains (BM), so progress can be accelerated towards achieving Sustainable Development Goals (SDGs) and eventually Sustainable Development (SD).

Materials and methods

Description of the study area

The present study was carried out in the Mezam division (Fig. 1) with Bamenda as the head quarter, the city capital of the North West region of Cameroon.

But the study area considered in this research work is the Bamenda Mountains chain forest (BMCF) or the Bamenda Mountains (BM). This area is between latitude 5°46′00″N to 5°56′30″N of the equator and longitude 10°10′00″E to 10°16′30″E of the Greenwich meridian, with an altitude of 2621 m. The Bamenda Mountains (BM) is situated exactly between Mount Bamboutos in the SW and Mount Oku in the NW with altitudes of 2740 m and 3011 m, respectively, all constituting the Western Highlands of Cameroon (WHC), along the Cameroon Volcanic Line (CVL) or Cameroon Line (CL) (Fig. 2). The BM is at the central part of the WHC, which is practically a continual volcanic structure with no clear cut demarcation between the mountains. This site (BM) has many geomorphological structures such as calderas, escarpments, volcanic dykes, steep slopes, domes, plateau, plains, and even valleys (Guedjeo et al., 2017; Zangmo et al., 2017; Chenyi et al., 2017; Dedzo et al., 2013) with two main calderas: Santa-Mbu and Lefo.

The topography of this site is accidental, originating from the variety of volcanic activities that have occurred. It also has a conducive tropical climate of two seasons: a long rainy season from March to October with a short dry season from November to


Legend:
North West Division
Région
NIGERIA
Extrême-Nord
Nord
Adamaoua
Nord-Ouest
Ouest
Sud Ouest
Centre
Littoral
Est
Sud
RCA
Source: INC 2011, MINTP 2013
Legend:
Mezam Subdivision
Division
NIGERIA
Menchum
Donga - Mantung
Boyo
Bui
Momo
Mezam
Ngo-Ketunjia
West
0 25 50 100 Kilometers
Source: INC 2011, MINTP 2013
Legend:
Subdivision Heard Quater
Division Heard Quater
Region Heard Quater
River
Road
National
Regional
Divisional
Rural
Subdivision
Division
Menchum
Boyo
Bafut
Njikwa
Mbengwi
Tubah
Bamenda 3
Bamenda 2
Bamenda
Bamenda 1
Momo
Mezam
Ngo-Ketunjia
Balikumbat
Bali
Batibo
Santa
West
Coordinate System: GCS WGS 1984
Datum: WGS 1984
Units: Degree
Source: INC 2011, MINTP 2013
Babadjou
Galim
0 5 10 20 Kilometers
10°E
10°10'E
10°20'E
6°10'N
6°N
5°50'N

◂**Fig. 1** Location map of the study area

February. Mean temperature is between 21 and 25 °C with annual rainfall between 1800 and 2500 mm (Guedjeo et al., 2017; Yufenyuy & Nguetsop 2020). Soils here are mostly lateralitic characterized with red color, also suitable for agricultural practices especially when properly irrigated and fertilized. The vegetation cover of the BM is mainly of savannah and forest types.

The Bamenda Mountains chain forest harbors many species of plants and animals. The plants present here are of great therapeutic values. The location of the Bamenda Mountains chain gives it a special importance. Like any other mountainous forest, this site is rich with abundant flora and fauna, goods and services to mankind. It is as well the source of many water bodies.

The CVL is the principal multifaceted plutono-volcanic passing through Cameroon. This volcanic line is 1600-km long and 100-km wide (Zangmo et al., 2017), extending from the Gulf of Guinea in the Atlantic ocean up to Lake Chad in the African continent (Fig. 3). Essential studies have highlighted that the CL is subjected to threats of diverse origins, and these milieus have pulled and encouraged an active population of diverse origins and nurtured their settlement during the past years (Dedzo et al., 2013; Wantim et al., 2013; Guedjeo et al., 2013; Zangmo et al., 2017).

Data acquisition and analysis

The data used in this research work were mainly imagery from remote sensing, topographic maps, and field observations. Data from GPS records (training sites and ground control points (150)) assisted in the process (Fig. 5). Related literatures as well and reconnaissance information assembled from the field of study (key informant interview and focus groups discussions) were also used. Several aerial images from Google Earth application were used as well to assist in the classification process. All relevant information was collected and analyzed in support of the issue being investigated. These data helped to compliment the methods used in the study. The satellite images used were downloaded from the United States Geological Survey (USGS) website (http://glovis.usgs.gov/).

The landscape dynamics was investigated using Landsat TM (thematic mapper), ETM+ (enhanced thematic mapper), and OLI-TIRS (operational land imager and thematic infrared sensor) singly captured in 1988, 2003, and 2022 (Table 1). The above remote sensing dataset used for the research work was cloud-free and of the dry season to ensure the land cover and mostly the vegetative cover which is the topic of the study could be perceived.

Image preprocessing and classification methods

ERDAS IMAGINE 11, ArcGIS 10, and IDRISI SELVA 17.0 software were used for this study to perform the image processing functions required to complete the land cover classification. Using this method, the area of interest (AOI) from all the land cover types in the image was extracted. The images of the study area were taken through three stages to generate land cover classes of the study area. These included:

– Feature identification using a spectral profile
– Choice of training data (signatures)
– Choice of appropriate classification methods

All images were atmospherically and geometrically corrected using ERDAS IMAGINE 11 to avoid haze, sensor noise, and to adjust loss or missing data due to the position of the sun and satellite calibration (Feranec et al., 2007; Tadese et al., 2021). The images were projected to UTM (Universal Transverse Mercator) zone 32 by the World Geodetic System 84 (WGS84) datum. Layer stacking, image subsetting, image enhancement, NDVI, BI, and color composite were performed on all the images of the study dates to make objects more visible to lessen omission and confusion errors and ensure more accuracy during the classification process (Wubie et al., 2016; WoldeYohannes et al., 2018; Temgoua et al., 2018).

The present study made use of a hybrid method of image classification (both unsupervised and supervised) using IDRISI SELVA 17.0, as summarized in Fig. 6. An unsupervised classification was to obtain main training parcels for field verification followed by a supervised classification through maximum likelihood algorithm for the classification (Temgou et al., 2018; Bufebo & Elias, 2021; Wang et al., 2021)

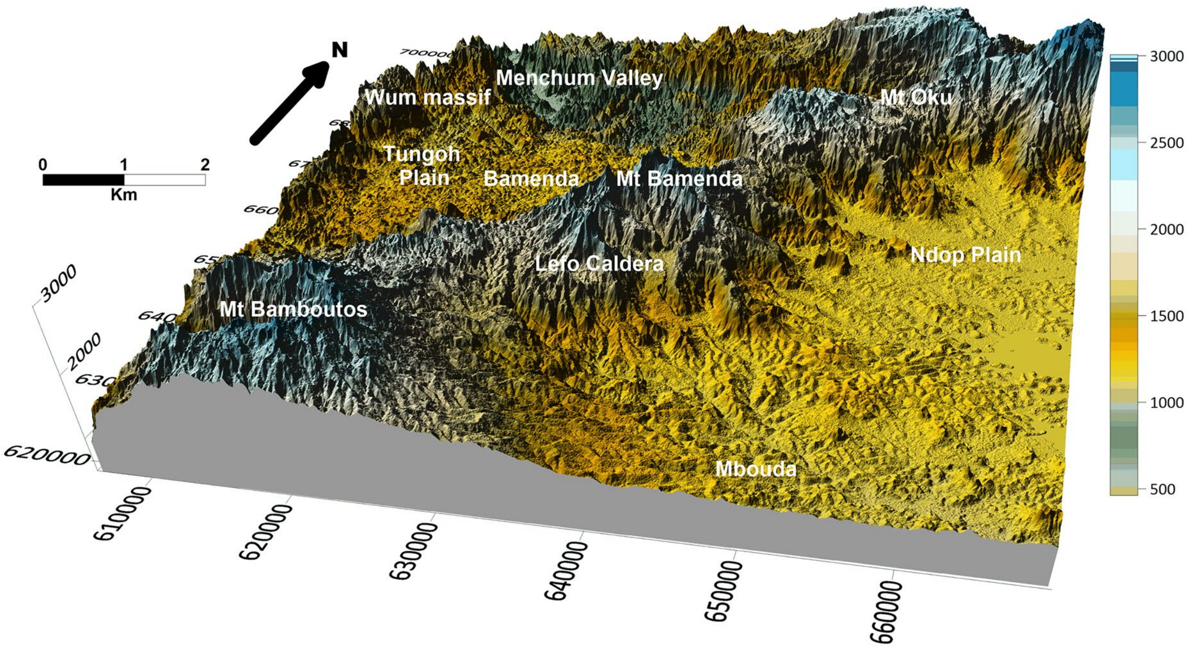

Fig. 2 The 3D map of Bamenda Mountains (MB), within the Western Highlands of Cameroon (WHC), adapted from Guedjeo et al. (2017)

of Landsat TM, ETM+, and OLI-TIRS images of the study dates. The above was followed by a time series analysis and prediction using IDRISI SELVA modeling.

After the classification of each image, they were imported into the ArcMap Catalogue package to generate maps used to compare each image date for better understanding the changes on the Bamenda Mountains chain over time. The classification technique adopted in this study was to make sure it suits the goal of the study. At the end, the LULC maps were derived with 6 classes.

Normalized Difference Vegetation Index (NDVI)

The NDVI which is the index of plant greenness was calculated for all the images of the study. The main reason for calculating this index was to support the image classification process. This index shows photosynthetically active vegetation, the amount of chlorophyll present in plant leaves, and thus an indication of vegetation quantity (Asong et al., 2019). The NDVI was gotten from the near-infrared (NIR) and the visible red light bands of the TM, ETM+, and OLI-TIRS satellite imageries of the study. Generally, photosynthetically active or abundant vegetation absorbs more incoming red light and reflects close to 25% of NIR, whereas scanty or unhealthy vegetation reflects most of the visible red light and less NIR light. The NDVI is calculated using the formula below (Asong et al., 2019):

$$\text{NDVI} = \frac{(NIR - RED)}{(NIR + RED)} \quad (1)$$

where NIR = near-infrared band value for a cell

RED = red band value for a cell

NDVI values range from −1 to +1 where values greater and positive indicate highly photosynthetically active vegetation or dense vegetation recorded by the sensor and negative or values less than zero have no ecological meaning they actually indicate non-vegetative classes (Weier & Herring, 2000).

Brightness Index (BI)

The Brightness Index (BI) characterizes the average of the brightness of a satellite image (Ouerchefani et al., 2009). It was computed using the formula below (Samiee et al., 2018).

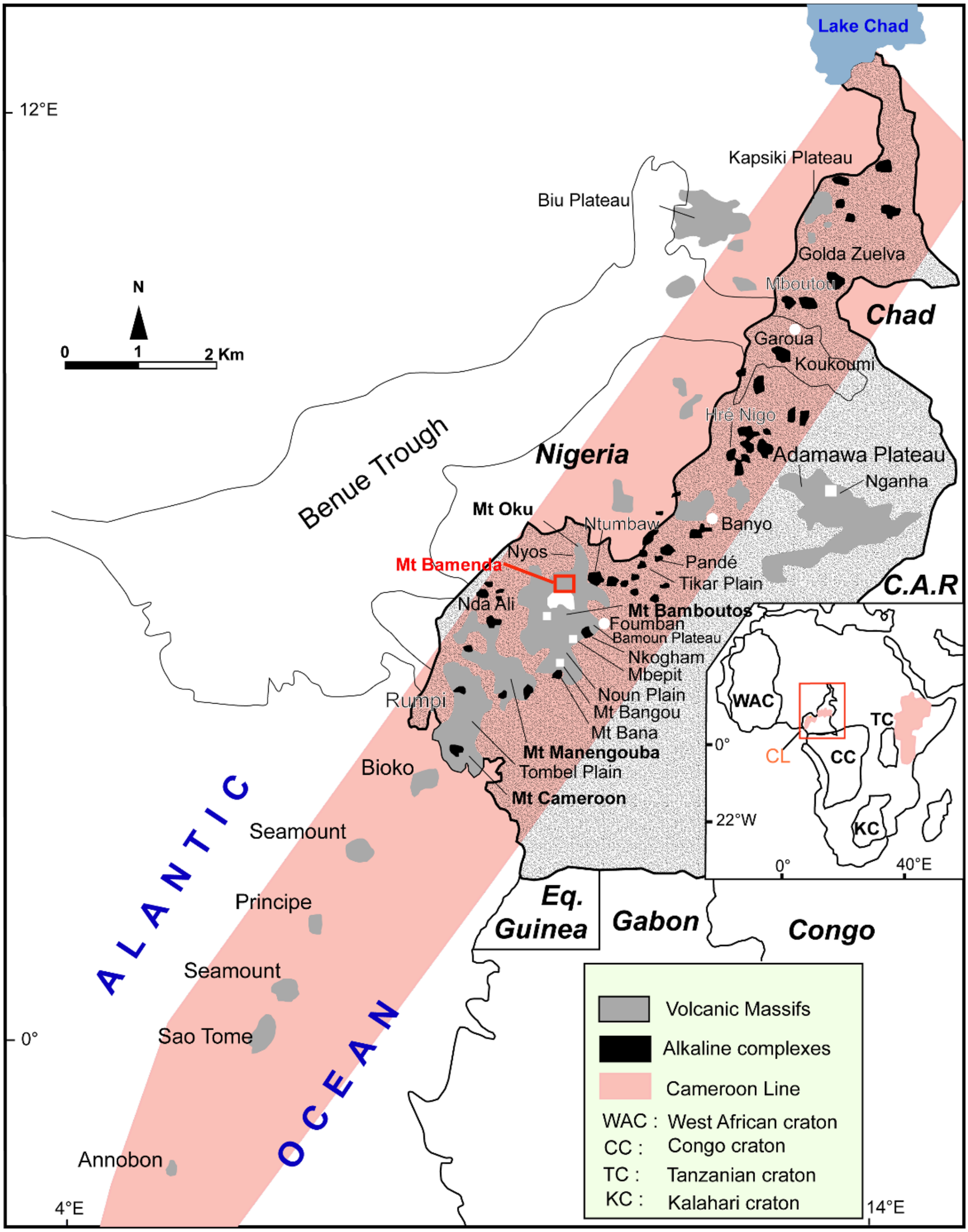

Fig. 3 Cameroon map showing the CVL and the location of MB within the WHC. Adapted from Zangmo et al. (2017)

$$BI = \sqrt{R^2 + NIR^2} \quad (2)$$

R = red band value for a cell

NIR = near infrared band value for a cell

The reason for the choice of the Normalized Difference Vegetation Index (NDVI) and Brightness Index (BI) was due to both indices having proven to be more reliable to effectively identify separate LULC categories of a study area (kolios and stylios, 2013).

Classification accuracy assessment

Assessing the classification accuracy is essential for the classified data to obviously detect changes (Wang et al., 2020, 2021). The accuracy assessment of the classified images was achieved using 150 Ground Control Points (GCP) (Fig. 5) recorded with the help of a hand held Garmin GPS, relevant information gathered via key informant interview, and focus group discussions. High-resolution Google Earth images (Fig. 4) and topographic maps were used as reference data to support the classification accuracy process (Fig. 6). Besides, field observations and personal knowledge about the study area also assisted. The classified images were compared to the reference data to understand the level of similarities and differences, helping to create an error matrix (Ariti et al., 2015; Bufebo & Elias, 2021).

The classification results of the data were cross-tabulated against the reference data to form the error matrices that helped to examine the classification accuracy. The producer's accuracy (omission error), user's accuracies (commission error), the overall accuracy, and kappa coefficient were calculated from the error matrices. Producer's accuracy was obtained by dividing the samples' number correctly identified by the totals of the reference data; meanwhile, the user's accuracy was gotten by dividing the samples' number correctly identified in each class by the classified totals (Ukrainshi, 2016; Said et al., 2021). The overall classification accuracy of each image of the study was calculated by dividing the pixels' number correctly classified by the total of the sample points (Ukrainshi, 2016; Said et al., 2021). The formula below (Bufebo & Elias, 2021) was used to calculate the overall accuracy.

$$A = \frac{X}{Y} * 100 \quad (3)$$

where A = overall accuracy

X = total of correct values in the diagonals of the matrix

Y = total of values of a reference point

The kappa coefficient is a measure of the total accuracy statistic of the error matrix between the classified map and the reference data. The said coefficient considers nondiagonal elements (Ukrainshi, 2016; Bufebo & Elias, 2021; Said et al., 2021). A value above 0.80 signifies a good classification; a value ranging from 0.40 to 0.80 signifies a moderate classification; and a value below 0.40 implies a poor classification (Firdaus, 2014) and thus implying the greater the kappa value, the authentic the classification (Ukrainshi, 2016). The formula below (Wang et al., 2021; Firdaus, 2014; Bufebo & Elias, 2021; Said et al., 2021) was used to calculate the kappa coefficient:

$$\mathrm{K} = \frac{N\sum_{i=1}^{r} xii - \sum_{i=1}^{r}(xi+ * x+i)}{N^2 - \sum_{i=1}^{r}(xi+ * x+i)} \quad (4)$$

where K = kappa coefficient

R = number of rows in matrix

Xii = number of observations in row i and column i

$Xi+$ = marginal totals of row i

$X+i$ = marginal total of column i

N = total of observations in the whole error matrix

Detection of land use and land cover change (LULCC)

The LULC changes in terms of hectares and percentages were calculated for all the study dates to understand the trends of change between land cover categories of the different study periods. The change detection was obtained from the formulas below (Hassen & Assen, 2018; Bufebo & Elias, 2021; Alemayehu, 2019):

$$\Delta e(\%) = \left(\frac{(X_2 - X_1)}{X_1} \right) * 100 \quad (5)$$

$$\Delta e \ rate = \left(\frac{ha}{year} \right) = \left(\frac{(X_2 - X_1)}{Y} \right) \quad (6)$$

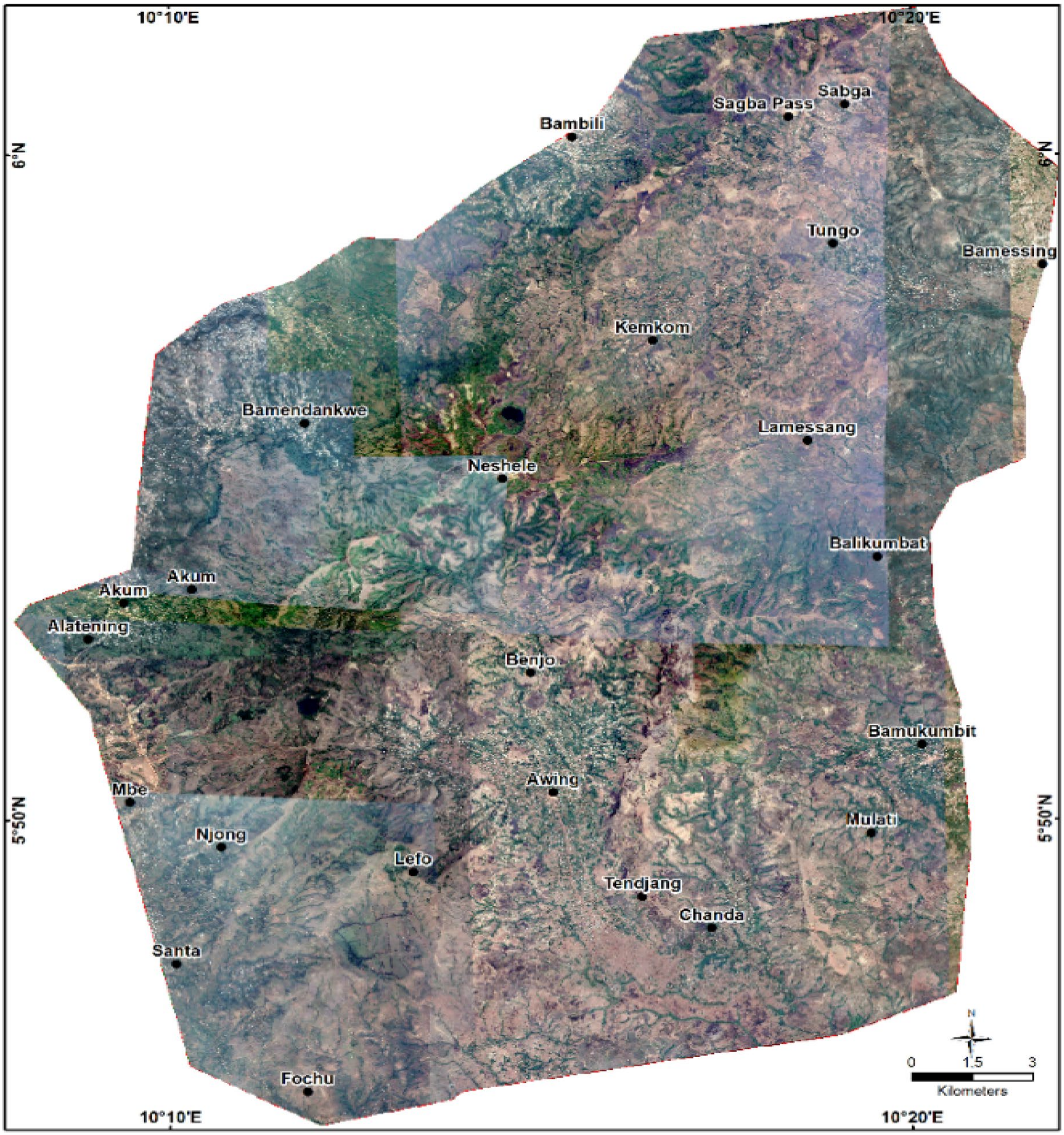

Fig. 4 Google image of the Bamenda Mountains, January 2021

where $\Delta e(\%)$ = percentage of change in LU area and LC type between initial time X_1 and final time X_2.

X_1 = LULC type at the initial year

X_2 = LULC type at the final year

Y = time interval between the final and initial years

Prediction of LULCC

Markov chain model which is a stochastic model, modeling temporal or sequential data, has been extensively used to model areas of land use changes at great spatial scales (Huang et al., 2008). The present study

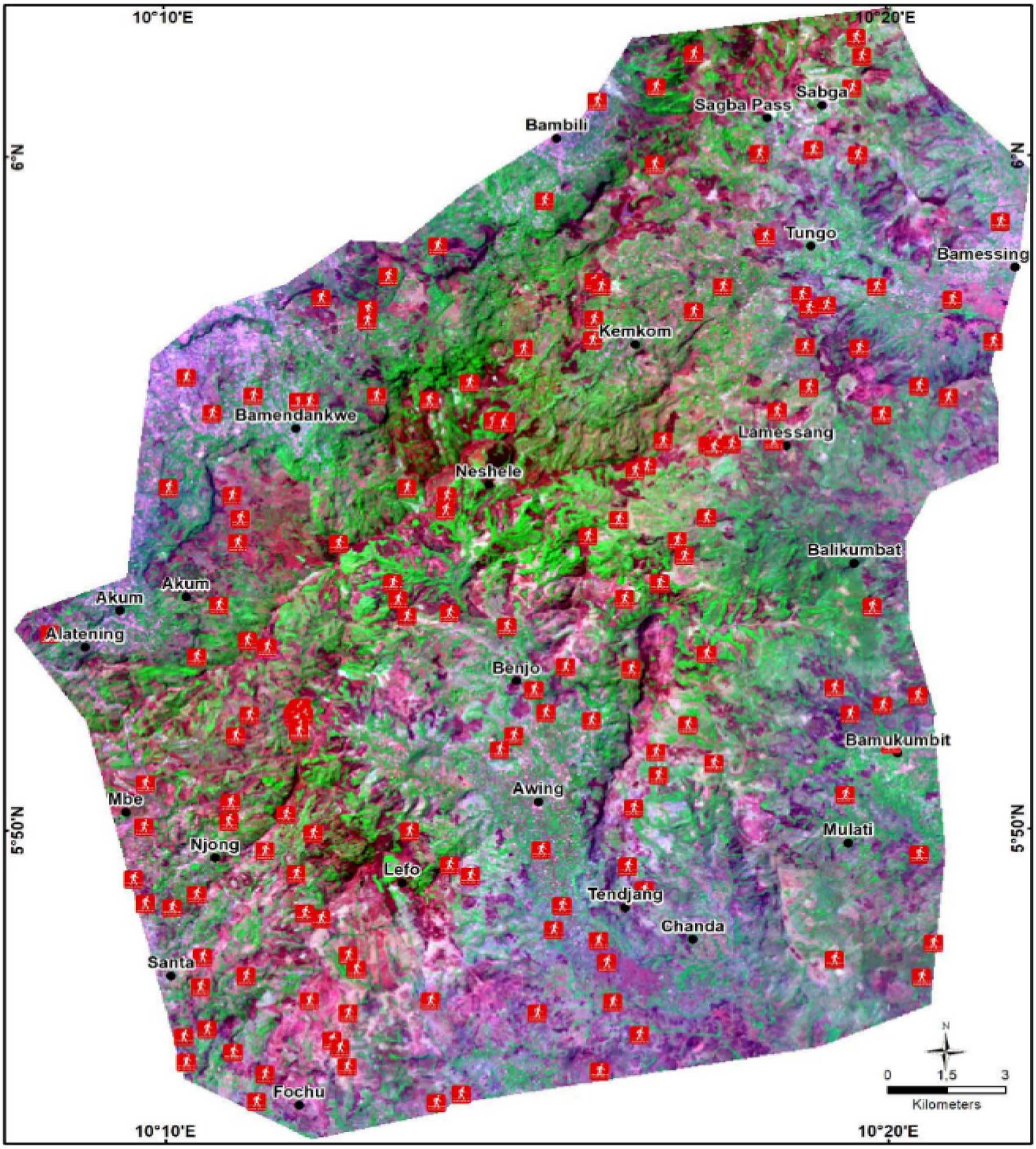

Fig. 5 Ground-truth activity in the Bamenda Mountains October 5–20, 2022

Table 1 Details of Landsat satellite images

Satellite image	Sensor	Acquisition date	Path/row	Resolution	Band	Source
Landsat 5	TM	1988/01/22	187/056	30*30m	6	USGS
Landsat 7	ETM+	2003/01/10	186/056	30*30m	8	USGS
Landsat 8	OLI-TIRS	2022/01/22	186/056	30*30m	11	USGS

made use of the Markov chain model (MCM) for time series analysis and prediction using IDRISI SELVA modeling where the land use change for the year 2056 was predicted. To achieve this objective, the 1988, 2003, and 2022, land cover maps were made using a maximum likelihood classification technique. From here, the land cover image (t-1) of 1988 and the land cover image (t = 1) of 2022 were considered to run a Markov model. This model generated both the transition probability file and the transition area file. The transition probability shows how a pixel is likely to change to a different LU and LC or remain the same in the subsequent time. But, a transition area matrix indicates a total area likely to change the subsequent time (Said et al., 2021). The results obtained from the Markov model joined with the suitability maps were used to run the CA-Markov model employing a 5 × 5 contiguity filter. From here, the simulated 2056 map was produced.

Transition suitability maps

The transitional suitability maps which show the probability of a pixel to change to another class or remain the same (Wang et al., 2021) were obtained using the multi-criteria evaluation (MCE). The MCE integration of various driving forces helps to develop the single index of evaluation (Wang et al., 2021, El-Hallaq & Habboub, 2014). The driving forces are different depending on the study area. The authors' good knowledge of the study area and the difficult nature of the terrain coupled with factors such as socio-economic, political, and physical closeness to existing LULC helped to determine the transition rules. The transition suitability maps were calculated using the distance to settlement areas, main road, cultivated areas, water bodies, and slopes. The digital elevation model (DEM) with road maps and other infrastructures was obtained from the Bamenda City Council. The standardized factor maps (0–1) were made using the fuzzy membership functions, with 0 representing unsuitable locations and 1 representing perfect locations. The weights of the driving forces were therefore derived from the analytic hierarchy process (AHP).

Prediction validation of LULCC

Model validation is primordial in the process of modeling (Said et al., 2021; Memarian et al., 2012). Studies (Baysal, 2013; Brown et al., 2013; Katana et al., 2013) have highlighted varieties of methods for

Table 2 Statistics of projection validation for 2022 reference and simulated LULC

	Information of quantity		
Information of allocation	No [n]	Medium [m]	Perfect [p]
Perfect[P(x)]	P(n) = 0.5783	P(m) = 0.9801	P(p) = 1.0000
PerfectStratum[K(x)]	K(n) = 0.5783	K(m) = 0.9801	K(p) = 1.0000
MediumGrid[M(x)]	M(n) = 0.5380	M(m) = 0.9523	M(p) = 0.9606
MediumStratum[H(x)]	H(n) = 0.1711	H(m) = 0.3192	H(p) = 0.3103
No[N(x)]	N(n) = 0.1711	N(m) = 0.3192	N(p) = 0.3103
	AgreementChance = 0.1711		
	AgreementQuantity = 0.1600		
	AgreementStrata = 0.0000		
	AgreementGridcell = 0.6732		
	DisagreeGridcell = 0.0378		
	DisagreeStrata = 0.0000		
	DisagreeQuantity = 0.0399		
K index	Kno = 0.9714		
K index	Klocation = 0.9506		
K index	KlocationStrata = 0.9506		
K index	Kstandard = 0.9247		

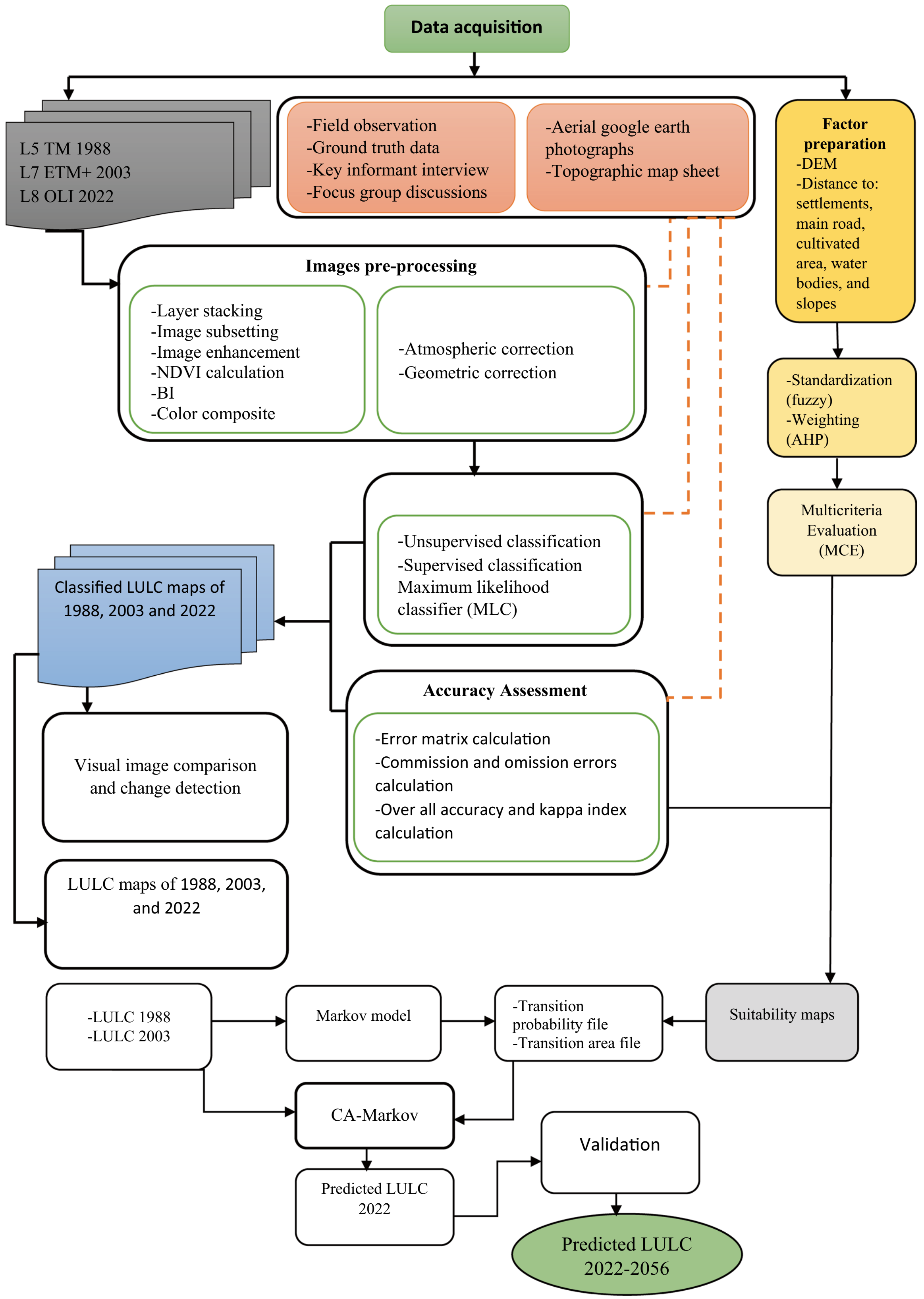
Data acquisition
L5 TM 1988
L7 ETM+ 2003
L8 OLI 2022
-Field observation
-Ground truth data
-Key informant interview
-Focus group discussions
-Aerial google earth photographs
-Topographic map sheet
Factor preparation
-DEM
-Distance to: settlements, main road, cultivated area, water bodies, and slopes
Images pre-processing
-Layer stacking
-Image subsetting
-Image enhancement
-NDVI calculation
-BI
-Color composite
-Atmospheric correction
-Geometric correction
-Standardization (fuzzy)
-Weighting (AHP)
Multicriteria Evaluation (MCE)
-Unsupervised classification
-Supervised classification Maximum likelihood classifier (MLC)
Classified LULC maps of 1988, 2003 and 2022
Accuracy Assessment
-Error matrix calculation
-Commission and omission errors calculation
-Over all accuracy and kappa index calculation
Visual image comparison and change detection
LULC maps of 1988, 2003, and 2022
-LULC 1988
-LULC 2003
Markov model
-Transition probability file
-Transition area file
Suitability maps
CA-Markov
Validation
Predicted LULC 2022
Predicted LULC 2022-2056

◂**Fig. 6** Flow chart of remote sensing methodology framework for the study

model validation such as chi-square and *F*-test of the observed and simulated images, the kappa coefficient and Cramer's *V*, as well as the quantity and allocation disagreements. To achieve the prediction validation results the present study made use of kappa index of agreement (KIA) technique using the VALIDATE module in IDRISI SELVA to examine the level of resemblance between the actual and simulated 2022 LULC. The above technique provided the validation statistics for the reference 2022 LULC and the comparison 2022 LULC (Table 2). The validation module observes the agreement between the LULC maps of the same classes (Gupta et al., 2020). The cross-tabulation approach was used to ascertain the magnitude of transformations of each LULC, for model validation after which the 2056 future LULC map was projected.

Results

Assessment of the classification accuracy of the classified 1988, 2003, and 2022

The kappa statistic is one of the effective and widely used methods of measuring the model capacity to predict (Hua, 2017; Wang et al., 2021). Studies (Viera & Garrett, 2005; Manonmani & Suganya, 2010) have also highlighted that a kappa value < 0 signifies no agreement; 0.01–0.20 implies slight; 0.21–0.40 as fair; 0.41–0.60 as moderate; 0.61–0.80 as significant; and 0.81–0.99 as nearly perfect agreement. For the present study to be reliable and accurate, the overall accuracy was computed for all the classified images of the study periods (1988, 2003, 2022) with values 95.83%, *94.25%*, and *94.48%*, kappa statistics values of 0.94, *0.91*, and *0.92,* respectively (Table 3). The above statistics thus show a reliable level of agreement for the study.

Analysis of LULC change of the Bamenda Mountain

By analyzing land use and land cover, we can comprehend important changes that have occurred on land like loss of biodiversity, degradation of the natural environment, and landscape configuration (Wang et al., 2021).

The classification techniques used in this study yielded 6 LULC classes: montane forest, savannah, cultivated area, bare area, built-up, and lake (Table 4). Accordingly, the landscape configuration of the study area can be easily perceived from 1988 to 2022 (Fig. 7, Table 5).

The present study demonstrated the effectiveness of remote sensing and GIS techniques in mapping, classifying, and finalizing the different land use and land cover categories of the Bamenda Mountains chain forest from 1988 to 2022. Looking at the analysis (Fig. 7, Table 5), it is readily perceived that the land cover types vary, followed by substantial alteration throughout the study period. The characteristics of these land cover classes are well explained at the research methodology section above (Table 4). The Bamenda Mountains occupy the northeastern and south western part of the map, presenting the

Table 3 Accuracy assessment and kappa coefficient of agreement of the classified images

LUC classes	L5 TM 1988		L7 ETM+ 2003		L8 OLI 2022	
	Producer's accuracy (%)	User's accuracy (%)	Producer's accuracy (%)	User's accuracy (%)	Producer's accuracy (%)	User's accuracy (%)
Lake	100.00	90.00	90.00	90.00	81.82	90.00
Savannah	98.80	97.59	98.02	96.12	98.67	94.87
Built-up	90.00	90.00	75.00	90.00	100.00	90.00
Forest	91.40	96.97	84.62	91.67	85.71	92.31
Cultivated A.	100.00	93.75	96.43	93.10	95.35	97.62
Bare A.	93.80	93.75	90.00	90.00	81.82	90.00
Overall accuracy	**95.83**%		**94.25**%		**94.48**%	
Kappa coefficient	**0.94**		**0.91**		**0.92**	

Bold simply signifies emphasis

Table 4 LULC classes for the study dates (1988–2022) and their descriptions

LULC classes	Descriptions
Montane forest	Area of dense vegetation, made up of both natural and planted forests, forming almost closed canopies, on the mountains
Built-up area	Areas occupied by commercial and residential buildings and transportation facilities
Savanna	Grassland areas with herbaceous plants, short and stunted trees, grazing fields
Cultivated area	Areas used for the growing of different types of crops
Bare area	Open landscape mainly rocky with little or no vegetative cover
Lake	Areas occupied by extensive standing or slowly moving water bodies

vegetation which is the main focus of interest in the study and other LULC categories. The montane forest (dense vegetation on mountain top) is gradually degraded followed by the savannah mainly on steep slopes. We also have both clustered and linear settlement patterns around towns (Bamenda and Bambili) confirming the saying that goes: "where the road passes, development follows" (Lim, 1999). Built-ups are as well scattered throughout the study area, with cultivated areas and bare areas at their proximities (Fig. 7). A small proportion of the surface area of the study site is covered by water notably lakes.

Overall, built-up and cultivated areas are all on the increase throughout the study period at the expense of other land cover types. These built-up areas (449 ha (0.83%); 996 ha (1.83%); 3242 (5.94%)) and cultivated areas (5684 ha (10.47%); 10680 ha (19.57%); 15163 (27.78%)) for the years 1988, 2003, and 2022, respectively (Table 5), can be justified by the population growth of the Mezam division. Population growth and its repercussions on the natural environment are common worldwide and severe in developing countries (Alemu et al., 2012). Likewise, the Mezam population is estimated at 5234.127 inhabitants, with around 86 persons per km^2, and when compared to the past, the population trend is on the increase. The rural population of this division depends mainly on agriculture and livestock rearing. With the increased human and livestock population, agricultural lands are on the increase at the detriment

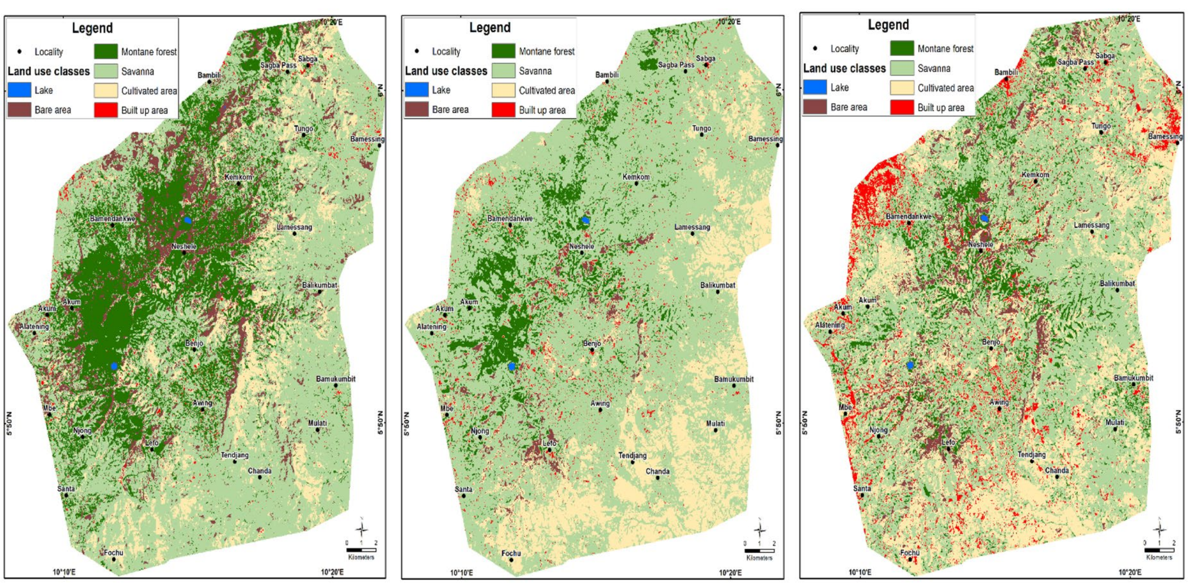

Fig. 7 LULC maps of 1988, 2003, and 2022

Table 5 Areas of LULC change of the Bamenda Mountains from 1988–2022

LULC classes	1988		2003		2022	
	Area (ha)	Area (%)	Area (ha)	Area (%)	Area (ha)	Area (%)
Bare area	5684	10.47	943	1.73	3215	5.89
Built up area	449	0.83	996	1.83	3242	5.94
Cultivated area	5684	10.47	10680	19.57	15163	27.78
Montane forest	12138	22.37	4509	8.26	4588	8.41
Savannah	30288	55.81	37416	68.56	28337	51.92
Lake	28	0.05	28	0.05	28	0.05
Total	**54271**	**100**	**54271**	**100**	**54271**	**100**

Bold simply signifies emphasis

of the natural environment. Looking at the forest vegetation, it can be seen that the montane forest dropped from 1988 to 2003 (12,138 ha (22.37%); 4509 ha (8.26%), respectively) with a slight increase in 2022 (4588 ha (8.41%)) as seen in (Table 5, Fig. 7). The sudden increase in montane forest from 2003 to 2022 could be attributed to the plantation of new trees under agroforestry projects and practices (Awazi et al., 2022). The savannah that occupied the highest surface area in 1988 (30288 ha (55.81%)) (Fig. 7, Table 5) dropped throughout the study period. Water body that occupied the smallest proportion of the study area remained unchanged throughout the study period. It is vital to underscore that the montane forest and the savannah vegetation somewhat dropped significantly during the study period at the expense of cultivated lands and built-up. Contrarily, bare soil dropped from 1988 to 2022 (5684 ha (10.47); 943 ha (1.73%), respectively) and considerably increased in 2022 (3215(ha) 5.89%). The sudden increase of bare area in the year 2022 could be attributed to cattle rearers' activities through grazing especially in Lefo, in the southern part of the study area and Neshele in the northern part of the study area. Both grazers and the farmers' activities through bush fires and expansion of agricultural lands play a vital role in the bare areas observed (Temgoua et al., 2018). The ongoing civil unrest in Cameroon otherwise known as the Anglophone crisis has played a significant role in the bare areas observed. The current conflictual civil war has led to massive destruction of properties and villages in the North West region of Cameroon (Amnesty International, 2021). As of 2018, reports on human right abuses indicates that around 87 villages have been burnt down in the North West region of Cameroon (Lee et al., 2021; U.S. House of Representatives, 2018). Current findings reveal that properties including houses are continually being ruined in over 170 villages (Agwanda et al., 2020; Bang et al., 2022).

Patterns of change of LULC of the Bamenda mountains for the past 34 years (1988–2022)

Overall, the LULCC results (Table 6, Fig. 8) indicate that built-up and cultivated lands increased throughout the study period (1988–2022). This implies that 5.11% and 17.31% of the total study area were occupied by built-up and cultivated land, respectively. The above patterns of LULC changes are attributed to the increase

Table 6 Percentage of change of LULC of the Bamenda Mountains

LULC classes	1988	2003	2022	Overall change (1988–2022)
Bare area	10.47%	1.73%	5.89%	4.58%
Built-up area	0.83%	1.83%	5.94%	5.11%
Cultivated area	10.47%	19.57%	27.78%	17.31%
Montane forest	22.37%	8.26%	8.41%	−13.96%
Savannah	55.81%	68.56%	51.92%	−3.89%
Lake	0.05%	0.05%	0.05%	0%

in the population trend of the Mezam division that necessitates the desire to expand agricultural lands and thus the occupation of marginal lands, at the detriment of the natural environment. Although bare area dropped in 2003 and significantly increased in 2022, the reasons for the sudden increase are livestock rearers' and farmers' activities. However, the civil unrest going on in Cameroon and particularly in the North West and South West regions as discussed in *the analysis of LULC change of the Bamenda Mountains* section above contributes in a greater extend to the bare areas observed.

The areas occupied by other land cover categories showed losses differently (Table 6, Fig. 8) throughout the study period, with the greatest losses experienced by the montane forest, followed by the savannah vegetation (−13.96%, −3.89%, respectively).

LULC transition between 1988 and 2022

To better understand the evolution of LULC categories of the Bamenda Mountain, six classes were mapped (Fig. 7), following the LULC transition between the study years (Fig. 9). The transition map was generated by the LCM and showed areas of changes of the classes from 1988 to 2022. It is obvious that the selected classes showed transitions differently from 1988 to 2022. The transition from savanna to cultivated area (9546.93 ha) is higher throughout the study period due to the population growth of the Mezam division. This was followed by the transition from forest to savannah (6550.65 ha). The most stable LULC category during the study period is cultivated area to bare area (302.31 ha), implying there is a low probability of cultivated area transitioning to bare area. The next stable category is cultivated area to built-up (489.06 ha), showing that the probability of cultivated area transitioning to built-up is also low. The transition from forest to bare area and from forest to cultivated land showed significant changes (513.36 ha, 1500.3 ha, respectively) and anthropogenic activities through deforestation, agricultural expansion, built-up, and cattle grazing are some of the main

Fig. 8 Patterns of change of LULC of the Bamenda Mountains with gains and losses form 1988 to 2022

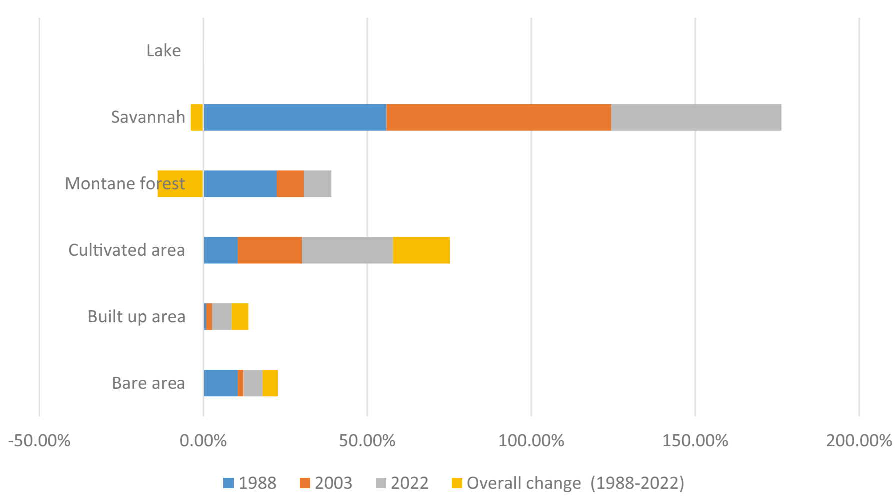

Table 7 The transition probability matrix of 2056 LULC change

Given : Probability to change to :	L	SV	BltA	MF	CA	BA
L	0.9243	0.0032	0.0032	0.0000	0.0000	0.0694
SV	0.0000	0.5470	0.0665	0.0371	0.3152	0.0341
BltA	0.0000	0.3019	0.5188	0.0032	0.1502	0.0258
MF	0.0000	0.5397	0.0231	0.2713	0.1236	0.0423
CA	0.0000	0.4253	0.0817	0.0023	0.4402	0.0505
BA	0.0002	0.4463	0.0394	0.0274	0.2489	0.2378

L = lake, *SV* = savanna, *BltA* = built-up area, *MF* = montane forest, *CA* = cultivated area, *BA* = bare area

factors responsible for the forest vegetation loss of the study area (Alemu et al., 2012; Temgoua et al., 2018). All the remaining LULC categories show great transitions differently (Fig. 10).

The transition probability matrix of 2056 LULC change

The probability of LULC of 2056 showed the dynamism of LULC classes (Table 7). Nevertheless, the likelihood of most classes remaining the same was high for lake (0.9243), savanna (0.5470), and built-up area (0.5188); cultivated area showed moderate likelihood of remaining the same (0.4402). However, the probability of other LULC categories to remain unstable was low. It is obvious from Table 7 that no LULC categories will change to lake.

Results revealed a higher probability of montane forest changing to savanna (0.5397), with moderate probability of cultivated area to savanna (0.4253) than savanna to cultivated area (0.3152). Values also showed a moderate probability of bare area changing to savanna (0.4463). The main reason for the conversion of montane forest could be increased population in the Mezam division, through immigration from neighboring subdivisions for greener pastures, especially as Bamenda is the head quarter of the North West region of Cameroon.

The projection results and validation of LULC of the Bamenda Mountain

The model accurately simulated the 2056 LULC (Fig. 11) by making a comparison of both the observed and simulated 2022 LULC maps. There was good similarity between their classes and the spatial distribution of classes (Table 8).

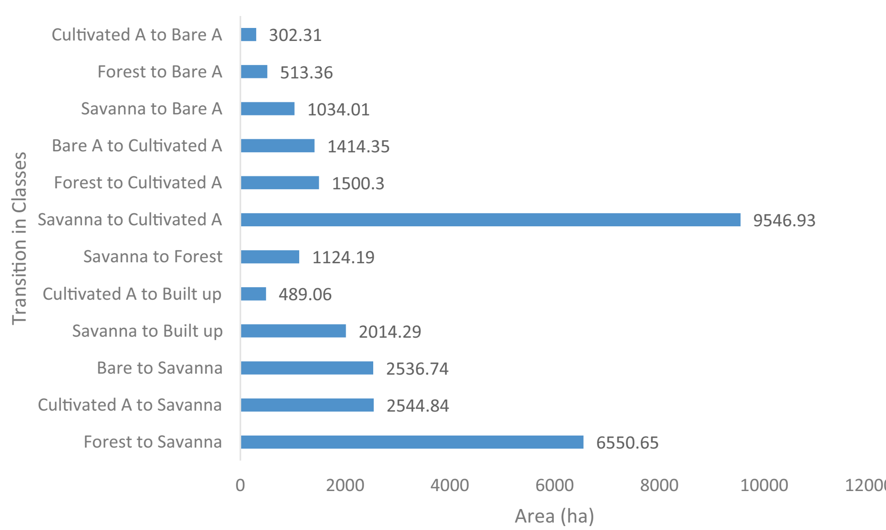

Fig. 9 Transition area in six LULC classes of the Bamenda Mountains from 1988 to 2022

Table 8 Predicted LULC for 2056

LULC classes	Area (ha)	Area (%)
Lake	28	0.05
Savanna	25862.67	47.39
Built-up area	6364.89	11.66
Montane forest	2401.92	4.40
Cultivated area	17008.56	31.17
Bare area	2905.92	5.32

Prediction validation of LULC

The prediction validation results were achieved using kappa index of agreement (KIA) technique, employing the VALIDATE module in IDRISI SELVA to examine the level of resemblance between the actual and simulated 2022 LULC. The above technique provided the validation statistics for the reference 2022 LULC and the comparison 2022 LULC (Table 2). The validation module observes the agreement between the LULC maps of the same classes (Gupta et al., 2020). The cross-tabulation approach was used to ascertain the magnitude of transformations of each LULC, for model validation after which the 2056 future LULC map was projected.

The model validation statistics (Table 2) show classification agreement/disagreement according to ability to specify accurately quantity and allocation. The statistics clearly pointed out the resemblance between the actual 2022 LULC and the comparison 2022 LULC. However, the dissimilarity between the two is due to the changes still to take place. The accuracy assessment statistics using the kappa coefficient variations confirms the authenticity of the classified images (Table 3). The overall accuracies were 95.83%, *94.25%*, and *94.48%* for 1988, 2003, and 2022 images, respectively. Likewise, the model showed the overall accuracy of the simulated map to be Kno, 97.14 %; Klocation, 95.06%; KlocationStrata, 95.06%; and Kstandard, 92.47%.

Expected transition in 2056 by surface area in hectares and percentage

The predicted LULC of the Bamenda Mountains using the Markov chain model is presented in Table 8 and Fig. 11. The 2056 LULC categories and surface areas were compared to those of 2022 to quantify the changes. The predicted figures of 2056 showed a continuous reduction of montane forest by 2401.92 ha (4.40%) and savanna by 25,862.67 ha (47.39%). Bare area is expected to drop in 2056 by 2905.92 ha (5.32%) (Table 2). The above decrease, when compared to 2022 figures (Table 6), represents a loss of 3.97%, 4.53%, and 0.57% for montane forest, savanna, and bare area, respectively. The losses observed are gained by built-up and cultivated land (5.72% and 3.39%, respectively), covering surface areas of 6364.89 ha (11.66%) and 17,008.56 ha (31.17%), respectively.

The 2056 spatial distribution of LULC (Fig. 11) shows that the montane forest scatters across the study area with more patches towards the northern part, the central part, and the western part of the study area. The patches of forest remaining are observed mostly at the proximity of cultivated land, built-up, and savanna. The land cover categories covered by vegetation will be converted to built-up and cultivated land by 2056. The above transition is due to population increase and urbanization in the North West region of Cameroon, which is similar to that of many less developed countries of the world (Alemu et al., 2012; Said et al., 2021).

Discussion

Land use/land cover change

Land use/land cover change (LULCC) poses severe threats to the climate system which further disrupts the ecological balance while inducing nefarious effects on human well-being (Gomes et al., 2021). While these changes can be assessed using a wide range of techniques, remote sensing and GIS offer a deep-rooted technology that helps to monitor, analyze, map, and forecast future land use scenario, to understand patterns of change in temporal and spatial aspects. The analysis of the LULCC of the Bamenda Mountains chain for the studied years (1988–2022) was computed, and LULC maps were generated. The overall accuracies obtained for Landsat TM (95.83%), ETM+ (94.25%), and OLI-TIRS (94.48%) for the years 1988, 2003, and 2022, respectively (Table 4) were authentic. Also, the kappa statistics for Landsat

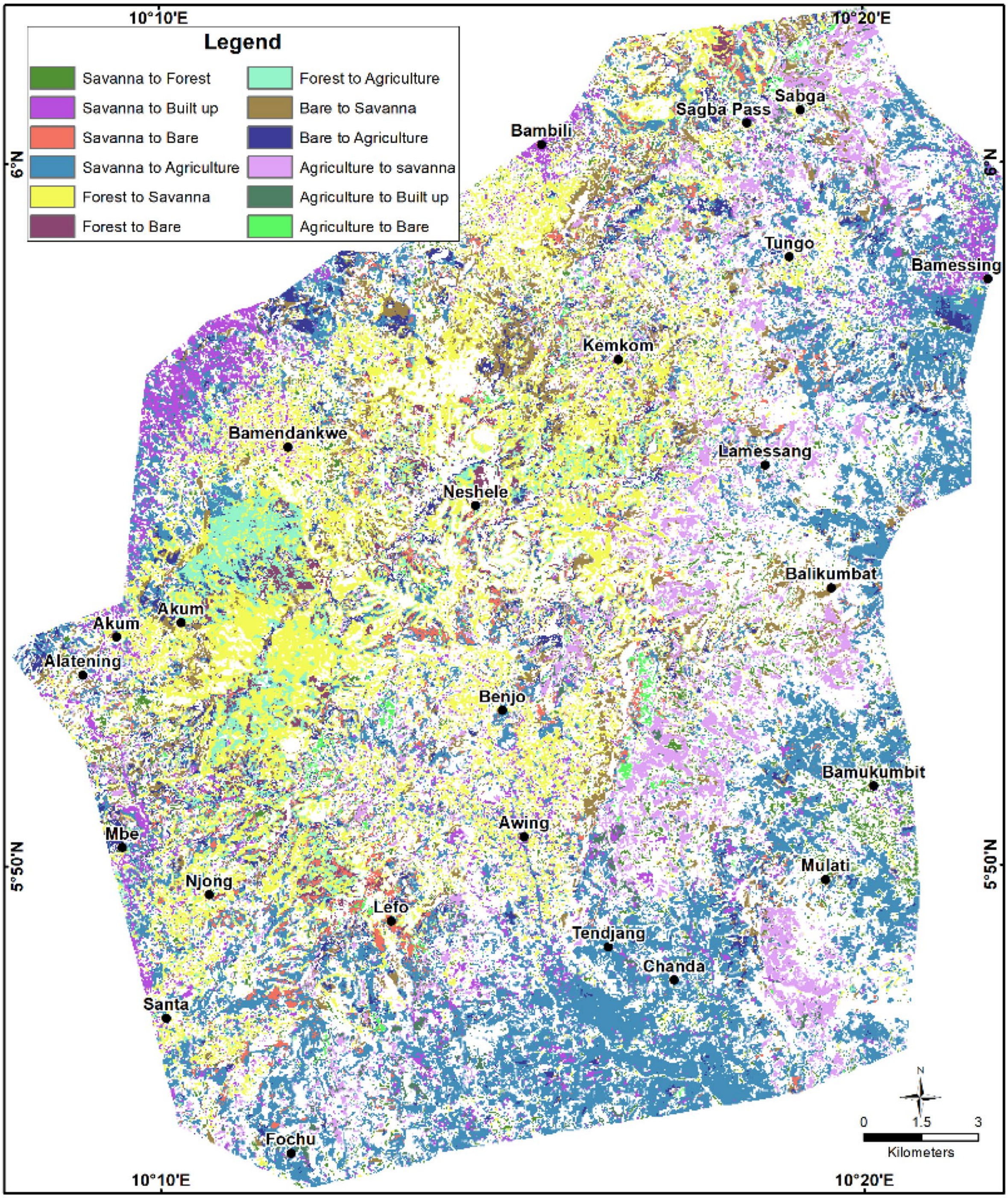

Fig. 10 LULC transition map of the Bamenda Mountains from 1988 to 2022

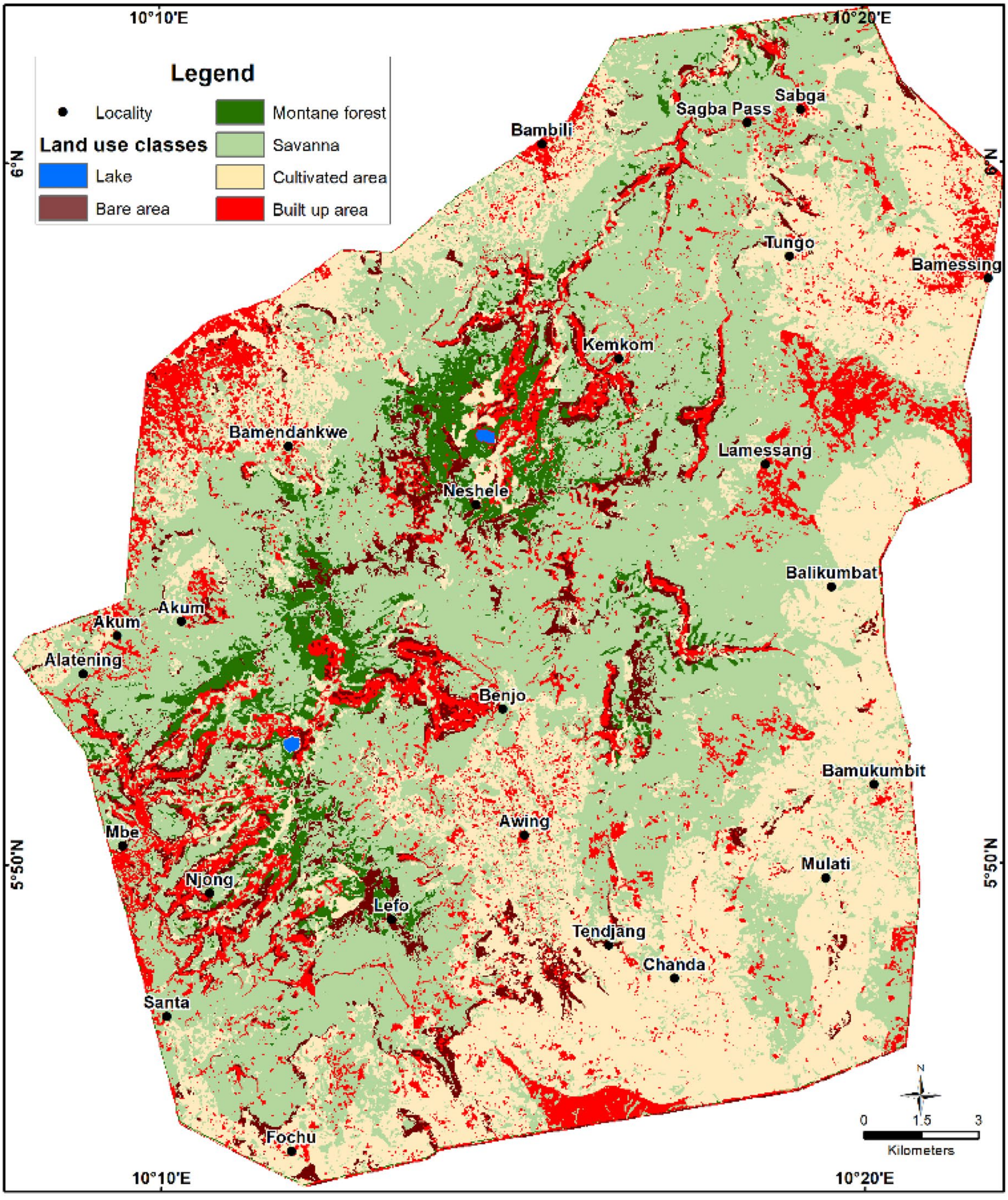

Fig. 11 Predicted LULC map of 2056

TM (0.94), ETM+ (0.91), and OLI-TIRS (0.92) for the years 1988, 2003, and 2022, respectively (Table 3), beefed up the accuracy and reliability of the study. The kappa coefficient and overall accuracies were above 90%, indicating a high level of satisfaction of the classification performance (Tadese et al., 2021; Lahon et al., 2023). These outcomes coincide with the current findings of Weslati et al. (2023) in the case of Mellengue catchment area of North Africa, and Akdeniz et al. (2023) in the case of Belek tourism center of Turkey.

Six LULC classes (Table 4) were mapped, and the resulting outcomes revealed they transitioned differently throughout the study period (1988–2022). For instance, the alteration from the natural vegetation to other land cover categories such as cultivated area (1500.3 ha), built-up (2014.29 ha), and bare area (513.36 ha) points to the diversity of underlying causes and the severity of land use intensity in Mezam. A wholesale of studies attribute LULC configuration to population growth (Ishtiaque 2017; Rimal et al., 2018; Wang et al., 2021) and meagerly to other factors. It is important to highlight that population growth has a multiplier effects on both human well-beings and the natural environment. Over the years, the Bamenda Mountains chain has been severely infringed by the rapidly growing population of Mezam division due to the constant quest for food, water, energy resource, construction material and other valuable resources. Additionally, just like in the entire country, over 70% of the active population in Mezam is involved in crop production and livestock-rearing activities (Awazi, 2022). Contextually, this area constitutes an integral part of Western Highlands of Cameroon habitually referred to as the breadbasket of the Central African sub-region, due to the great quantity of food and cash crop production in the region (Kimengsi et al., 2022). However, population expansion raises alarms regarding the effects of urbanization and the invasion of marginal lands due to urban sprawl, resulting to the configuration of the natural landscape that may potentially compromise food security in Mezam and across the national territory. Nevertheless, these configurations do not come as a surprise as such trends are not new in many developing countries of the world (Bruggeman et al., 2016; Wang et al., 2021). As long as the transformation of the natural land to agricultural fields (dominant activity of the area) comes with livelihood benefits, future land use changes are inevitable. Therefore, investments in agriculture within Mezam division and across the national territory should take into account sustainable environmental practices like agroforestry by incorporating fast growing trees like *Sesbania sesban* and *Calliandra calothyrsus* amid crops. This suggestion aligns with Awazi and Tchamba (2019) who highlighted agroforestry as a climate change mitigation strategy for smallholder farmers in the North West region of Cameroon. To complement this action, the urban population should be educated on the need to embrace renewable energy usage. These actions serve as a blueprint to fulfilling the social responsibility of reducing carbon dioxide emissions which goes in line with sustainable development goals “Goal 7: Ensure access to affordable, reliable, sustainable and modern energy for all” and “Goal 13: Take urgent action to combat climate change and its impacts” (Matte et al., 2015; Sachs et al., 2022; Jan et al., 2023).

Patterns of change of land use and land cover

The shrinkage of the vegetation cover from 1988 to 2022 to the benefits of built-up and agricultural lands comes with detrimental impacts on the natural environment. For instance, the increase in cultivated land and the built-up area (Fig. 7, Table 5) throughout the study period is linked to the population growth trends of Bamenda. Studies highlight that population growth goes in line with the occupation of marginal lands due to urbanization (Hyandye & Martz, 2017, Amgoth et al., 2023). Increased population also skyrockets food demand, thus the expansion of agricultural lands (Said et al., 2021). Human encroachment into the forest and the replacement of the forest vegetation by settlements and crop lands are also reported in mountainous areas of the North West region of Cameroon (Maghah et al., 2021; Fogwe et al., 2019). The above results necessitate the visitation of regulations and laws governing forests and protected areas in Cameroon. Recent studies on LULC change mostly at the frontiers of protected areas put forward the need for more research and policymakers to revise policies and ensure their execution in protected areas (Tesfaw et al., 2018; Said et al., 2021).

Future land use and land cover change

In Cameroon, varied empirical studies have assessed LULC changes across different regions (Ewane and Lee, 2020; Ewane et al., 2023; Siwe & Koch, 2008; Mertens & Lambin, 2000), but only few of such works foretold future LULC scenarios (Moskolai et al., 2022; Saputra and Lee, 2019). In like manner, several studies have uncovered the spatio-temporal dynamics of LULC in the North West region of Cameroon with emphasis on watershed management (Temgoua et al., 2018), ecological changes (Mofor et al., 2022), and spatio-temporal NDVI (Maghah et al., 2021), while others relate spatio-temporal alternations to protected zones and agro-pastoral conflicts (Ntangti et al., 2019). However, none of these studies considered predicting the future land use scenarios of this region, thus validating the relevance of the current study. By assessing the status and spatio-temporal dynamics of the Bamenda Mountains while forecasting future land use scenarios, this study will bring clarity and closure to prolonged debates surrounding land use change in the North West region of Cameroon and other tropical mountainous ecosystems.

Markov chain model utilized in this research is a stochastic framework, modeling temporal or sequential data that has been widely used to display areas of land use changes at great spatial scales (Huang et al., 2008). This model, with the help of the transition probability matrix, shows how possible one LULC category can change into another LULC category (Vazquez-Quintero et al., 2016; Halmy et al., 2015). CA-Markov chain model is more appropriate for land use and land cover change prediction (Camara, 2020; Subedi et al., 2013; Kumar et al., 2014). This model is suitable especially when the changes and the direction of the changes are complex to define. This model is an appropriate fit for the Bamenda Mountains chain forest, as this zone is a multi-faceted pluto-volcanic structure with no clear cut demarcation between its mountains (Zangmo et al., 2017; Wantim et al., 2013). The model validation of the current study using the kappa index of agreement (KIA) compared the simulated and the actual 2022 LULC map. The KIA statistics (Table 2) showed a high level of resemblance between the simulated and the actual 2022 LULC map. The overall accuracies (95.83%, 94.25%, and 94.48% for 1988, 2003, and 2022 images, respectively) and the overall kappa index of agreement (Kno, 97.14%; Klocation, 95.06 %; KlocationStrata, 95.06%; and Kstandard, 92.47%) indicated a high level of agreement standards between the simulated and actual 2022 LULC map (Gashaw et al., 2017; Singh et al., 2015; Mosammam et al., 2017). The CA-Markov chain model thus proved to be a reliable and an effective tool to predict and analyze the 2056 LULC changes. The 2056 figures showed a great reduction of the vegetation cover (montane forest and savanna) at the expense of built-up area and cultivated land (Table 8, Fig. 11). These results are in line with the findings of Gashaw et al. (2017) in the Blue Nile Basin of Ethiopia; Yirsaw et al. (2017) in the coastal area of Su-Xi Chang in China; and Liping et al. (2018) in a hilly landscape of Jiangle in China. The expansion of agricultural lands and settlement at the detriment of the natural environment (Table 8,) everything being equal, could be attributed to future anthropogenic activities due to future population growth. The 2056 predicted LULC could be used as a guide for decision-makers, land use management planners, and conservationists of the study area for sustainable land management.

Conclusion and recommendations

Analyses of land use and land cover change (LULCC) are essential to inform decision-makers on planning policy of land use. There have been significant LULCC of the Bamenda Mountains, in the North West region of Cameroon. Following the field observations, the Ground Control Points collected, the key informant interview, and focus group discussions, the changes observed on this site are largely attributed to population pressure and livestock rearing. The main finding of the present research work revealed a substantial change of the Bamenda Mountains for the past 34 years (1988–2022). Cultivated land and built-up all increased throughout the study period at the expense of the vegetation cover that shrank drastically. The predicted figures of 2056 showed a continuous reduction of montane forest and savanna 2401.92 ha (4.40%) and 25,862.67 ha (47.39%), respectively. Bare area is expected to drop in 1956 (2905.92 ha (5.32%)). The above decrease, when compared to 2022 figures, represents a loss of 3.97%, 4.53%, and 0.57%, respectively. The losses observed are gained by built-up and cultivated land (5.72% and 3.39%, respectively), covering surface areas of 6364.89 ha (11.66%) and 17,008.56 ha (31.17%), respectively.

The vegetation cover of the study area is expected to continue reducing. In 2056, montane forest, savanna, and bare area are expected to drop by 3.97%, 4.53%, and 0.57%, respectively, when compared to the 2022 figures, whereas the shrinkage observed will be gained by built-up and cultivated land (5.72%

and 3.39%, respectively). The direction of LULCC viewed by the respondents was concordant with the satellite image interpretation results. The main driving forces of the Bamenda Mountains change are anthropogenic activities. This implies that, ecosystem alteration, loss of biodiversity, and the deterioration of forest products are likely to continue with disastrous consequences on the environment and the livelihood of the local community. Nevertheless, the bird life study in the Kilum Ijim Forest reserve of Oku in the North West region of Cameroon suggests suites of bird species to be indicators of vegetation changes. Remote sensing and GIS technology are thus a reliable, competitive, and cost-effective technology having the potentials to map out, obtain information, and analyze land use changes from large portions of the earth over long periods.

To ensure the sustainable management of the environment of this site, improved land conservation techniques, afforestation and reforestation, and off-farm activities are crucial. Also, organizing campaigns of education and information to sensitize the general public of the Mezam division is possible. Ensuring clear land tenure policies in the North West region in particular and in Cameroon at large is essential for land management planning.

The civil conflict in the North West and South West regions of Cameroon has been considered a human right crisis by the international community, given it emanated from the marginalization of the Anglophones through gradual infiltration of the French educational and legal systems into the English systems. The root cause of the crisis may be traced back to violating the 1961 constitution that bind both parties with equal status. Meanwhile, the civil unrest in the North West and South West regions constitutes one of the causes of landscape configuration in both regions.

This conflictual civil war needs an immediate intervention. This could be possible through a genuine and inclusive dialogue between leaders of the opposing parties (the state and Anglophone leaders) in a neutral land (outside Cameroon) and in the presence of international mediators (UNO, Cameroons' colonial powers and other countries with strong bilateral ties with Cameroon). Human rights should be respected; thus, Anglophone detainees and those already imprisoned should be released and given a chance to participate in the dialogue. A disarmament committee with representatives from both parties should facilitate the ceased fire process.

Satisfying these three measures can build confidence and trust amongst the parties concerned and the general population. Then, upon settling for a gentleman agreement, a reconstruction committee can rebuild the affected regions. This may not happen overnight. However, it could be the gateway out of the crisis and a starting point to landscape reconstruction in the region.

Future scholars could consider the effect of civil conflicts on landscape dynamics in the North West and South West regions of Cameroon. Also, analyzing the relationship between landscape configuration and land tenure is crucial, as the tenure in place favors the haphazard occupation of land in the North West region of Cameroon.

Acknowledgements The authors are wholeheartedly grateful to all the anonymous reviewers from whom this paper largely benefited. Our appreciation equally goes to all the respondents and to the Bamenda City Council for their hospitality and good morality. We remain indebted to Pr. Paul TEMATIO for his retain less support, valuable criticisms, and suggestions, for dedicating his time and expertise to assist with GIS and remote sensing techniques in spite of his heavy schedules.

Declarations All authors have read, understood, and have complied as applicable with the statement on "ethical responsibilities of authors" as found in the Instructions for Authors and are aware that with minor exceptions, no changes can be made to authorship once the paper is submitted.

All authors certify that they have no affiliations with or involvement in any organization or entity with any financial interest or non-financial interest in the topic or materials discussed in this manuscript.

Competing interests The authors declare no competing interests.

Author contribution Kongni Fopa Virgiline: research design, conceptualization, methodology, software, data processing, analysis, and manuscript writing. Devrim ÖZDAL: supervision, visualization, investigation, and reviewing. Nihal Bayir: co-supervision, guidance, and proofreading the final manuscript. The final manuscript was edited, read, and approved by all authors.

Data availability The authors confirm that the data supporting the findings of this research are available within the manuscript. Additional information about the dataset used could be obtained from the corresponding author upon reasonable request.

References

Agwanda, B., Nyadera, I. N., & Asal, U. Y. (2020). Cameroon and the Anglophone crisis. *The Palgrave Encyclopedia of Peace and Conflict Studies*, 1–11. https://doi.org/10.1007/978-3-030-11795-5_115-1

Ahlcrona, E. (1989). *The impact of climate and man on land transformation in Central Sudan. Applications of remote sensing* (No. 103).

Akdeniz, H. B., Sag, N. S., & Inam, S. (2023). Analysis of land use/land cover changes and prediction of future changes with land change modeler: Case of Belek, Turkey. *Environmental Monitoring and Assessment, 195*(1), 135.

Alemayehu, F., Tolera, M., & Tesfaye, G. (2019). Land use land cover change trend and its drivers in Somodo watershed south western, Ethiopia. *African Journal of Agricultural Research, 14*(2), *102–117*.

Alemu, M., Suryabhagavan, K. V., & Balakrishnan, M. (2012). Assessment of cover change in the Harenna habitats in Bale Mountains, Ethiopia, using GIS and remote sensing. *International Journal of Ecology and Environmental Sciences, 38*, 39–45.

Amgoth, A., Rani, H. P., & Jayakumar, K. V. (2023). Exploring LULC changes in Pakhal Lake area, Telangana, India using QGIS MOLUSCE plugin. *Spatial Information Research*, 1–10. https://doi.org/10.1007/s41324-023-00509-1

Amnesty International. (2021). *Cameroon: Witness testimony and satellite images reveal the scale of devastation in Anglophone regions*. Retrieved September 11, 2022, from https://www.amnesty.org/en/latest/press-release/2021/07/cameroon-satellite-images-reveal-devastation-in-anglophone-regions/

Ariti, A. T., van Vliet, J., & Verburg, P. H. (2015). Land-use and land-cover changes in the Central Rift Valley of Ethiopia: Assessment of perception and adaptation of stakeholders. *Applied Geography, 65*, 28–37.

Asaha, S., & Deakin, E. L. (2016). *Land-use change and its influence on rural livelihoods, food security and biodiversity conservation in the Southwest Region of Cameroon* (pp. 54–90). Agrarian change in tropical landscapes. Center for International Forestry Research (CIFOR), Bogor, Indonesia.

Asong, T. V., Yerima, B., & P., K., Che Bih V. (2019). An Assessment of land-use and land-cover dynamics using Normalized Difference Vegetation Index (NDVI) in North West Cameroon. *Open Access Journal of Environmental and Soil Sciences, 3*(4). https://doi.org/10.32474/OAJESS.2019.03.000166

Awazi, N. P., & Tchamba, N. M. (2019). Enhancing agricultural sustainability and productivity under changing climate conditions through improved agroforestry practices in smallholder farming systems in sub-Saharan Africa. *African Journal of Agricultural Research, 14*(7), 379–388.

Awazi, N. P., Tchamba, M. N., Temgoua, L. F., & Tientcheu-Avana, M. L. (2022). Agroforestry as an adaptation option to climate change in Cameroon: Assessing farmers' preferences. *Agricultural Research, 11*(2), 309–320.

Bang, H. N., & Balgah, R. A. (2022). The ramification of Cameroon's Anglophone crisis: conceptual analysis of a looming "Complex Disaster Emergency". *Journal of International Humanitarian Action, 7*(1), 1–25. https://doi.org/10.1186/s41018-022-00114-1

Baysal, G. (2013). *Urban land use and land cover change analysis and modeling a case study area Malatya*. Turkey. Master's Thesis, Institute for Geoinformatics (IFGI), Westfälische Wilhelms-Universität, Münster.

Brown, D. G., Band, L. E., Green, K. O., Irwin, E. G., Jain, A., Lambin, E. F., Pontius, R. G., Seto, I. I. K. C., Turner, A., & Verburg, P. H. (2013). *Advancing land change modeling: Opportunities and research requirements*. N. A. Press.

Bruggeman, D., Meyfroidt, P., & Lambin, E. F. (2016). Forest cover changes in Bhutan: Revisiting the forest transition. *Applied Geography, 67*, *49–60*.

Bufebo, B., & Elias, E. (2021). Land use/land cover change and its driving forces in Shenkolla Watershed, South Central Ethiopia. *The Scientific World Journal, 2021*. https://doi.org/10.1155/2021/9470918

Camara, M., Jamil, N. R. B., Abdullah, A. F. B., & Hashim, R. B. (2020). Integrating cellular automata Markov model to simulate future land use change of a tropical basin. *Global Journal of Environmental Science and Management, 6*(3), 403–414.

Chen, A., Yang, X., Guo, J., Zhang, M., Xing, X., Yang, D., et al. (2022). Dynamic of land use, landscape, and their impact on ecological quality in the northern sand-prevention belt of China. *Journal of Environmental Management, 317*, 115351.

Chenyi, M. L. V., Nkouathio, D. G., Wotchoko, P., Nono, G. D. K., Zenon, I., Guedjeo, C. S., & Seuwui, D. T. (2017). Volcanology and geochemical study of the volcanic rocks of the Bafmeng area (Mount Oku, Cameroon Volcanic Line). *International Journal of Biological and Chemical Sciences, 11*(2), *941–964*.

Dedzo, M. G., Kamgang, P., Njonfang, E., Tefogoum, G. Z., Dongmo, A. K., & Nkouathio, D. G. (2013). Mapping and assessment of volcanic hazards related to the ignimbritic eruption by AMS in Bambouto Volcano (Cameroon Volcanic Line). *The Open Geology Journal, 7*(1), 1–13.

El-Hallaq, M. A., & Habboub, M. O. (2014). Using GIS for time series analysis of the Dead Sea from remotely sensing data. *Open Journal of Civil Engineering, 4*(04), 386.

Ewane, E. B., Deh-Nji, A., Mfonkwet, N. Y., & Nkembi, L. (2021). Agricultural expansion and land use land cover changes in the Mount Bamboutos landscape, Western Cameroon: implications for local land use planning and sustainable development. *International Journal of Environmental Studies.* https://doi.org/10.1080/00207233.2021.2006911

Ewane, B. E., & Lee, H. H. (2020). Assessing land use/land cover change impacts on the hydrology of Nyong River Basin. *Cameroon. Journal of Mountain Science, 17*(1), 50–67. https://doi.org/10.1007/s11629-019-5611-8

Ewane, E. B., Deh-Nji, A., Mfonkwet, N. Y., & Nkembi, L. (2023). Agricultural expansion and land use land cover changes in the Mount Bamboutos landscape, Western Cameroon: implications for local land use planning and sustainable development. *International Journal of*

Environmental Studies, 80(1), 186–206. https://doi.org/10.1080/00207233.2021.2006911
FAO. (2017). *Mountains and sustainable development goals*. Retrieved September 15, 2022, from http://www.fao.org/fileadmin/templates/mountain_partnership/doc/Mountains_and_the_SDGs.pdf
Feranec, J., Hazeu, G., Christensen, S., & Jaffrain, G. (2007). Corine land cover change detection in Europe (case studies of the Netherlands and Slovakia). *Land Use Policy, 24*(*1*), *234–247*.
Firdaus, R. (2014). Assessing land use and land cover change toward sustainability in humid tropical watersheds, Indonesia (Doctoral dissertation, 広島大学 (Hiroshima University)). From remotely sensing dat. *Open Civil Engineering Journal, 4*, *386–396*.
Fogwe, Z. N., Tume, S. J. P., & Fouda, M. (2019). Eucalyptus tree colonization of the Bafut-Ngemba Forest Reserve, North West Region, Cameroon. *Environment & Ecosystem Science, 3*(2), 12–16.
Forboseh, P. F., Keming, E. C., Toh, C. L., & Wultof, I. N. (2003). Monitoring of Kilum-Ijim forest bird communities: Initial findings. *Bird Conservation International, 13*(3), 255–271.
Gashaw, T., Tulu, T., Argaw, M., & Worqlul, A. W. (2017). Evaluation and prediction of land use/land cover changes in the Andassa watershed, Blue Nile Basin. *Ethiopia. Environmental Systems Research, 6*(1), 1–15.
Gomes, E., Inácio, M., Bogdzevič, K., Kalinauskas, M., Karnauskaitė, D., & Pereira, P. (2021). Future land-use changes and its impacts on terrestrial ecosystem services: A review. *Science of The Total Environment, 781*, 146716.
Gratzer, G., & Keeton, S. W. (2017). Mountain forests and sustainable development: The potential for achieving the United Nations' 2030 Agenda. *Mountain Research and Development, 37*(3), 246–253. https://doi.org/10.1659/MRD-JOURNAL-D-17-00093.1
Guedjeo, C. S., Kagou Dongmo, A., Ngapgue, F., Nkouathio, D. G., Zangmo Tefogoum, G., Gountié Dedzo, M., & Nono, A. (2013). Natural hazards along the Bamenda escarpment and its environs: The case of landslide, rock fall and flood risks (Cameroon volcanic line, North-West Region). *Global Advanced Research Journal of Geology and Mining Research, 2*(*1*), *15–26*.
Guedjeo, C. S., Kagou Dongmo, A., Wotchoko, P., Nkouathio, D. G., Chenyi, M. L., Wilson Buma, G., & Kamgang, K. V. (2017). Landslide susceptibility mapping and risk assessment on the Bamenda Mountain (Cameroon Volcanic Line). *Journal of Geosciences and Geomatics, 5*(4), 173–185.
Gupta, R., & Sharma, L. K. (2020). Efficacy of spatial land change Modeler as a forecasting indicator for anthropogenic change dynamics over five decades: A case study of Shoolpaneshwar Wildlife Sanctuary, Gujarat, India. *Ecological Indicators, 112*, 106171. https://doi.org/10.1016/j.ecolind.2020.106171
Halmy, M. W. A., Gessler, P. E., Hicke, J. A., & Salem, B. B. (2015). Land use/land cover change detection and prediction in the north-western coastal desert of Egypt using Markov-CA. *Applied Geography, 63*, 101–112.
Hassen, E. E., & Assen, M. (2018). Land use/cover dynamics and its drivers in Gelda catchment, Lake Tana watershed, Ethiopia. *Environmental Systems Research, 6*(1), 1–13.
Hua, A. K. (2017). Landuse land cover changes in detection of water quality: A study based on remote sensing and multivariate statistics. *Journal of Environmental and Public Health, 2021*. https://doi.org/10.1155/2017/7515130
Huang, W., Liu, H., Luan, Q., Jiang, Q., Liu, J., & Liu, H. (2008). Detection and prediction of land use change in Beijing based on remote sensing and GIS. *Int*. *The International Archives of the Photogrammetry, Remote Sensing and Spatial Information Sciences, 37*, *75–82*.
Hyandye, C., & Martz, L. W. (2017). A Markovian and cellular automata land-use change predictive model of the Usangu Catchment. *International Journal of Remote Sensing, 38*(1), 64–81.
Ishtiaque, A., Shrestha, M., & Chhetri, N. (2017). Rapid urban growth in the Kathmandu. *Environments, 4*(4), 72.
Jan, A. A., Lai, F. W., Asif, M., Akhtar, S., & Ullah, S. (2023). Embedding sustainability into bank strategy: Implications for sustainable development goals reporting. *International Journal of Sustainable Development & World Ecology, 30*(3), 229–243.
Katana, S., Ucakuwun, E., & Munyao, T. (2013). Detection and prediction of land cover changes in Upper Athi River Catchment, Kenya: A strategy towards monitoring environmental changes. *Greener Journal of Environmental Management and Public Safety, 2*(4), 146157. https://doi.org/10.15580/GJEMPS.2013.4.052113625
Kibreab, G. (1996). *People on the edge in the horn: Displacement, landuse and the environment in the Gedaref region, Sudan*. James Currey Ltd, Oxford, UK and the red Sea Press Inc, USA.
Kidane, Y., Stahlmann, R., & Beierkuhnlein, C. (2012). Vegetation dynamics, and land use and land cover change in the Bale Mountains, Ethiopia. *Environmental Monitoring and Assessment, 184*(12), 7473–7489. https://doi.org/10.1007/s10661-011-2514-8
Kimengsi, J. N., Akumbo, C. M., Balgah, R. A., Tingum, E. N., Tume, S. J. P., & Akhere, G. S. (2022). Farm-based climate adaptation dynamics: Insights from the vegetable sector in the Western Highlands of Cameroon. *Cogent Social Sciences, 8*(1), 2126452.
Kindu, M., Schneider, T., Teketay, D., & Knoke, T. (2013). Land use/land cover change analysis using object-based classification approach in Munessa-Shashemene Landscape of the Ethiopian Highlands. *Remote Sensing, 5*(5), 2411–2435.
Kolios, S., & Stylios, C. D. (2013). Identification of land cover/land use changes in the greater area of the Preveza peninsula in Greece using Landsat satellite data. *Applied Geography, 40*, 150–160.
Kumar, S., Radhakrishnan, N., & Mathew, S. (2014). Land use change modelling using a Markov model and remote sensing. *Geomatics, Natural Hazards and Risk, 5*(2), 145–156.
Lahon, D., Sahariah, D., Debnath, J., Nath, N., Meraj, G., Kumar, P., et al. (2023). Assessment of ecosystem service value in response to LULC changes using geospatial techniques: A case study in the Merbil Wetland of the

Brahmaputra Valley, Assam, India. *ISPRS International Journal of Geo-Information, 12*(4), 165.

Lee, S., Nganji, J. T., & Cockburn, L. (2021). Using twitter to understand the effects of the cameroon anglophone crisis on social determinants of health. *Medicine, Conflict and Survival, 37*(3), 221–247.

Leh, M., Bajwa, S., & Chaubey, I. (2013). Impact of land use change on erosion risk: An integrated remote sensing, geographic information system and modeling methodology. *Land Degradation & Development, 24*(5), 409–421.

Leumbe, O. L., Bitom, D., & Assako, R. J. (2012). *Évaluation des pertes en terres en région de montagne tropicale humide (cas du massif volcanique des Bambouto - Ouest Cameroun)*. https://doi.org/10.4000/books.irdeditions.13859

Lim, K. Y. (1999). *The role of road infrastructures in the tropical forests of Malaysia. In Road Infrastructures in Tropical Forests*. Food and Agriculture Organisation.

Liping, C., Yujun, S., & Saeed, S. (2018). Monitoring and predicting land use and land cover changes using remote sensing and GIS techniques—A case study of a hilly area, Jiangle. *China. PloS one, 13*(7), e0200493.

Lupo, F., Reginster, I., & Lambin, E. F. (2001). Monitoring land-cover changes in West Africa with SPOT vegetation: Impact of natural disasters in 1998–1999. *International Journal of Remote Sensing Sens, 22, 2633–2639*.

Maghah, J. A., Lambi, C. M., & Ambebe, T. F. (2021). Ecological change detection in Northeastern Bamenda Highlands, Cameroon, based on spatio-temporal Normalized Difference Vegetation Index (1979-2020). *European Journal of Environment and Earth Sciences, 2*(4), 5–10.

Mainguet, M. (2012). *Desertification: Natural background and human mismanagement*. Springer Science & Business Media.

Manonmani, R., & Suganya, G. M. D. (2010). Remote sensing and GIS application in change detection study in urban zone using multi temporal satellite. *International journal of Geomatics and Geosciences, 24, 60–65*.

Matte, S., Moyer, L., Kanuri, C., Petretta, D., Bulger, C., & Swaney, R. (2015). *Getting started with the sustainable development goals*. A Guide for Stakeholders. Columbia University's School of International and Public Affairs.

Mattsson, B. J., Mateo-Tomás, P., Aebischer, A., Rösner, S., Kunz, F., Schöll, E. M., et al. (2022). Enhancing monitoring and transboundary collaboration for conserving migratory species under global change: The priority case of the red kite. *Journal of Environmental Management, 317*, 115345.

Memarian, H., Balasundram, S. K., Talib, J. B., Sung, C. T. B., Sood, A. M., & Abbaspour, K. (2012). Validation of CA-Markov for simulation of land use and cover change in the Langat Basin, Malaysia. *Journal of Geographic Information System, 4(6), 542–554*. https://doi.org/10.4236/jgis.2012.46059

Mertens, B., & Lambin, E. F. (2000). Land-cover-change trajectories in southern Cameroon. *Annals of the association of American Geographers, 90*(3), 467–494. https://doi.org/10.1111/0004-5608.00205

Mofor, G. Z., Neo, K. P. G., & Ajoh, A. M. J. (2022). Conservation balance between man's need and ecological functions in Ajei Forest Area, Momo Division, Cameroon. *Journal of Geography, Environment and Earth Science International, 26*(6), 54–64.

Mosammam, H. M., Nia, J. T., Khani, H., Teymouri, A., & Kazemi, M. (2017). Monitoring land use change and measuring urban sprawl based on its spatial forms: The case of Qom city. *The Egyptian Journal of Remote Sensing and Space Science, 20*(1), 103–116.

Moskolai, W. R., Abdou, W., & Dipanda, A. (2022). A comparative study of deep learning and CA-Markov methods for land use/land cover change prediction. In *In 2022 16th International Conference on Signal-Image Technology & Internet-Based Systems (SITIS)* (pp. 190–197). IEEE. https://doi.org/10.1109/SITIS57111.2022.00043

Ntangti, F. C., Fokeng, R. M., Manu, I. N., & Gam, A. T. (2019). Land cover changes, protected areas and Agro-Pastoral Conflicts in Menchum, North West Cameroon. *American Journal of Humanities and Social Sciences Research, 3*, 41–50.

Olagunju, E. G. (2008). *Remote sensing for agricultural land use changes and sustainability monitoring in Sudan*. Digitala Vetenskapliga Arkivet. LIU-IDA/FFK-UP-A--08/021—SE.

Ouerchefani, D., Dhaou, H., Abdeljaoued, S., Delaitre, E., & Callot, Y. (2009). Radiometric indices for monitoring soil surfaces in South Tunisia. *Journal of Arid Land Studies, 19*(1), 73–76.

Rimal, B., Zhang, L., Keshtkar, H., Haak, B. N., Rijal, S., & Zhang, P. (2018). Land use/land cover change dynamics and modeling of urban land expansion by the integration of cellular automata and Markov chain. *ISPRS International Journal of Geo-Information, 7, 1–21*.

Rindfuss, R. R., Walsh, S. J., Turner, B. L., Fox, J., & Mishra, V. (2004). Developing a science of land change: Challenges and methodological issues. *Proceedings of the National Academy of Sciences of the United States of America, 101*, 13976–13981.

Sachs, J., Kroll, C., Lafortune, G., Fuller, G., & Woelm, F. (2022). *Sustainable development report 2022*. Cambridge University Press.

Said, M., Hyandye, C., Komakech, H. C., Mjemah, I. C., & Munishi, L. K. (2021). Predicting land use/cover changes and its association to agricultural production on the slopes of Mount Kilimanjaro, Tanzania. *Annals of GIS, 27*(2), 189–209.

Samiee, M., Ghazavi, R., Pakparvar, M., & Vali, A. A. (2018). Mapping spatial variability of soil salinity in a coastal area located in an arid environment using geostatistical and correlation methods based on the satellite data. *Desert, 23*(2), 233–242.

Saputra, M. H., & Lee, H. S. (2019). Prediction of land use and land cover changes for north Sumatra, Indonesia, using an artificial-neural-network-based cellular automaton. *Sustainability, 11*(11), 3024. https://doi.org/10.3390/su11113024

Shiferaw, A., & Singh, K. L. (2011). Evaluating the land use and land cover dynamics in Borena Woreda South Wollo Highlands, Ethiopia. *Ethiopian Journal of Business and Economics (The), 2*(1).

Simula, M. (2009). Towards defining forest degradation: Comparative analysis of existing definitions. *Forest Resources Assessment Working Paper, 154*, 59.

Singh, S. K., Mustak, S., Srivastava, P. K., Szabó, S., & Islam, T. (2015). Predicting spatial and decadal LULC changes through cellular automata Markov chain models using earth observation datasets and geo-information. *Environmental Processes, 2*, 61–78.

Siwe, R. N., & Koch, B. (2008). Change vector analysis to categorise land cover change processes using the tasselled cap as biophysical indicator. *Environmental Monitoring & Assessment, 145*. https://doi.org/10.1007/s10661-007-0031-6

Subedi, P., Subedi, K., & Thapa, B. (2013). Application of a hybrid cellular automaton–Markov (CA-Markov) model in land-use change prediction: A case study of Saddle Creek Drainage Basin, Florida. *Applied Ecology and Environmental Sciences, 1*(6), 126–132.

Tadese, S., Soromessa, T., & Bekele, T. (2021). Analysis of the current and future prediction of land use/land cover change using remote sensing and the CA-Markov model in Majang forest biosphere reserves of Gambella, southwestern Ethiopia. *The Scientific World Journal, 2021*. https://doi.org/10.1155/2021/6685045

Tematio, P. (2016). *Distribution of duricrusted bauxites and laterites on the Bamiléké plateau (West Cameroon): Constraints from GIS mapping and geochemistry*. Retrieved March 18, 2022, from https://www.researchgate.net/publication/291351420_Distribution_of_duricrusted_bauxites_and_laterites_on_the_Bamileke_plateau_West_Cameroon_Constraints_from_GIS_mapping_and_geochemistry

Temgoua, L. F., Ajonina, G., & Woyu, H. B. (2018). Land use and land cover change analysis in Ajei upland watershed community forest, North West Region, Cameroon. *Journal of Geoscience and Environment Protection, 6*(*9*), *83–99*.

Tesfaw, A. T., Pfaff, A., Golden Kroner, R. E., Qin, S., Medeiros, R., & Mascia, M. B. (2018). Land-use and land-cover change shape the sustainability and impacts of protected areas. *Proceedings of the National Academy of Sciences, 115*(*9*), *2084–2089*. https://doi.org/10.1073/pnas.1716462115

U.S. House of Representatives (2018). *Crisis in the republic of Cameroon, subcommittee on Africa, global health, global human rights, and international organizations of the committee on foreign affairs house of representatives one hundred fifteenth congress second session*. Retrieved May 20, 2023, from http://www.foreignaffairs.house.gov/, http://docs.house.gov, or http://www.gpo.gov/fdsys/

Ukrainshi, P. (2016). CLASSIFICATION ACCURACY ASSESSMENT. CONFUSION MATRIX METHOD. http://www.50northspatial.org/classification-accuracy-assessment-confusion-matrix-method/ Published 23/09/2016 | 3 | 47190| SCGIS, Remote Sensing valley, Nepal: monitoring land use land cover dynamics of a Himalayan city with

UN DESA. (2017). *World population projected to reach 9.8 billion in 2050, and 11.2 billion in 2100*. UN DESA| United Nations Department of Economic and Social Affairs, News.

Vázquez-Quintero, G., Solís-Moreno, R., Pompa-García, M., Villarreal-Guerrero, F., Pinedo-Alvarez, C., & Pinedo-Alvarez, A. (2016). Detection and projection of forest changes by using the Markov Chain Model and cellular automata. *Sustainability, 8*(3), 236.

Viera, A. J., & Garrett, J. M. (2005). Understanding interobserver agreement: the kappa statistic. *Family Medicine, 37*(*5*), *360–363*.

Wang, S. W., Munkhnasan, L., & Lee, W. K. (2021). Land use and land cover change detection and prediction in Bhutan's high altitude city of Thimphu, using cellular automata and Markov chain. *Environmental Challenges, 2*, 100017.

Wang, S. W., Gebru, B. M., Lamchin, M., Kayastha, R. B., & Lee, W. K. (2020). Land use and land cover change detection and prediction in the Kathmandu district of Nepal using remote sensing and GIS. *Sustainability*, *122–118*.

Wantim, M. N., Kervyn, M., Ernst, G. G. J., Del Marmol, M.-A., Suh, C. E., & Jacobs, P. (2013). Morpho-structure of the 1982 lava flow field at Mount Cameroon Volcano, West-Central Africa. *International Journal of Geosciences, 4*, *564–583*.

Weier, J., & Herring, D. (2000). *Measuring Vegetation (NDVI & EVI)*. NASA Earth Observatory.

Weslati, O., Bouaziz, S., & Sarbeji, M. M. (2023). Modelling and assessing the spatiotemporal changes to future land use change scenarios using remote sensing and CA-markov model in the mellegue catchment. *Journal of the Indian Society of Remote Sensing, 51*(1), 9–29.

WoldeYohannes, A., Cotter, M., Kelboro, G., & Dessalegn, W. (2018). Land use and land cover changes and their effects on the landscape of Abaya-Chamo Basin, Southern Ethiopia. *Land, 7*(*1*), *2*.

Wubie, M. A., Assen, M., & Nicolau, M. D. (2016). Patterns, causes and consequences of land use/cover dynamics in the Gumara watershed of lake Tana basin, Northwestern Ethiopia. *Environmental Systems Research, 5*(*1*), *1–12*.

Yirsaw, E., Wu, W., Shi, X., Temesgen, H., & Bekele, B. (2017). Land use/land cover change modeling and the prediction of subsequent changes in ecosystem service values in a coastal area of China, the Su-Xi-Chang Region. *Sustainability, 9*(7), 1204.

Yufenyuy, M., & Nguetsop, F. V. (2020). Climate Variability and the Emergence of Malaria: Case of Kumbo Central Sub-Division, North West Region, Cameroon. *International Journal of Global Sustainability, 4*(*1*), *104–127*. https://doi.org/10.5296/ijgs.v4i1.17263

Zangmo, G. T., Kagou, A. D., Nkouathio, D. G., Gountié, M. D., & Kamgang, P. (2017). The volcanic geoheritage of the Mount Bamenda calderas (Cameroon line): assessment for geotouristic and geoeducational purposes. *Geoheritage, 9*(3), 255–278.

Publisher's note Springer Nature remains neutral with regard to jurisdictional claims in published maps and institutional affiliations.

Springer Nature or its licensor (e.g. a society or other partner) holds exclusive rights to this article under a publishing agreement with the author(s) or other rightsholder(s); author self-archiving of the accepted manuscript version of this article is solely governed by the terms of such publishing agreement and applicable law.